Contents lists available at ScienceDirect

Marine and Petroleum Geology

journal homepage: www.elsevier.com/locate/marpetgeo

Depositional record of confined turbidites in syn-subduction intraslope basin: Insight from the Tufiti di Tusa Formation (Southern Apennines, Italy)

Salvatore Gallicchio [a,*], Davide Cerone [a], Roberto Tinterri [b]

[a] Department of Earth and GeoEnvironmental Sciences, University of Bari Aldo Moro, Campus Universitario, Via E. Orabona 4, 70125, Bari, Italy
[b] Department of Chemistry, of Life Sciences and Environmental Sustainability – Earth Sciences Unit, University of Parma, Parco Area delle Scienze 157/A, 43124, Parma, Italy

ARTICLE INFO

Keywords:
Facies analysis
Contained-reflected beds
Slurry beds
Trench-slope basin
Tectonics and sedimentation
Late Paleogene
Syn-orogenic volcanic deposits

ABSTRACT

A detailed lithostratigraphy and facies analysis of a type section of the Tufiti di Tusa Formation, including deep-marine clastic successions with syn-orogenic volcanic detritus and deposited in the late Eocene - early Miocene basin system at the front of the growing Maghrebian - Southern Apennines orogen, is discussed in the paper. Based on facies analysis and composition, the study section was subdivided into the following units, from bottom to top: Unit I, mostly formed by contained-reflected beds (including a bed similar to the Contessa megabed of the Marnoso-arenacea Formation in the Northern Apennines), with the ratio of sandstone intervals to mudstone intervals (S/M) of 0.6 and with mostly-calciclastic sandstone to siltstone fraction; Unit II, recording a moderate decrease in contained-reflected beds and a moderate increase in slurry beds, with S/M ratio of 0.9, and with mostly-siliciclastic sandstone to siltstone fraction; Unit III, recording a further decrease in contained-reflected beds and an evident increase in slurry beds and very-thick beds with a basal massive very coarse to coarse-grained sandstone, with S/M ratio of 2.5, and with mostly-volcaniclastic sandstone to siltstone fraction.

In accordance with the depositional models for the infill of confined turbidite basins, Units I and II are here interpreted as representing a flow ponding depositional phase, while Unit III as iconic of a flow stripping depositional phase. The compositional variation from Unit I to Unit II records cutoff of calciclastic supply from underplate sources, possibly tied to tectonic uplift of the external basin margin; while that from Unit II to Unit III records sudden availability of volcaniclastic sediment possible due to burial of morphological high(s) between the internal volcanic arc (source of the volcaniclastic sediment) and the depositional basin, and/or establishment of tectonically-controlled conduits cutting the above high(s). This study may improve the knowledge not only of infilling evolution of confined turbidite basins, but also the depositional setting of the late Paleogene Southern Apennines subduction margin in the Central Mediterranean.

1. Introduction

Deep-marine clastic systems are a major target for both the scientific community and the oil industry. In the last decades, a large number of experimental works (e.g., Pantin and Leeder, 1987; Kneller, 1995; Mulder and Alexander, 2001; Morris and Alexander, 2003; Brunt et al., 2004; Patacci et al., 2015; Soutter et al., 2021) and outcrop studies (e.g., Pickering and Hiscott, 1985; Haughton, 1994; Kneller, 1995; Remacha et al., 2005; Muzzi Magalhaes and Tinterri, 2010; Patacci et al., 2014; Tinterri and Tagliaferri, 2015; Tinterri et al., 2016, 2020, 2022; Bell et al., 2018; Cornard and Pickering, 2020; Cerone et al., 2021) have shown the fundamental role of basin topography in controlling the development of the deep-marine systems. A wide spectrum of features have been discussed, such as high bed thickness and peculiar sedimentary structures, such as biconvex ripples with sigmoidal-cross laminae, hummocky-type structures, convolute laminae and load structures, undescribed within the classical sequence of Bouma (1962), due to flow reflection, deflection and ponding processes (e.g. Pickering and Hiscott, 1985; Remacha et al., 2005; Tinterri, 2011; Tinterri et al., 2016, 2022 with references); reversal of paleocurrent directions within the same bed, which can be interpreted as the result of flow reflection and deflection processes (e.g. Pickering and Hiscott, 1985; Haughton, 1994; Remacha et al., 2005; Muzzi Magalhaes and Tinterri, 2010; Tinterri and Tagliaferri, 2015; Tinterri et al., 2016, 2022 with references).

* Corresponding author.
E-mail address: salvatore.gallicchio@uniba.it (S. Gallicchio).

https://doi.org/10.1016/j.marpetgeo.2022.105969
Received 25 June 2022; Received in revised form 5 October 2022; Accepted 8 October 2022

Active tectonics is certainly fundamental in producing basin-topography modifications and changes in sediment supplies (e.g., Bouma, 2004; Pickering and Hiscott, 2015; McArthur et al., 2022), and consequently is a primary factor influencing the depositional characteristics of deep-marine systems (e.g., Sinclair and Tomasso, 2002; Smith, 2004; DeCelles, 2012; Tinterri and Muzzi Magalhaes, 2011; McArthur et al., 2021).

The Tufiti di Tusa Formation (TTF; APAT, 2007 with references) is generally discontinuously scattered across the allochthonous sheets of the Lucanian Apennines and the Nebrodi Mountains (Southern Italy), but exceptionally shows excellent exposures, which enable analysis of how and when the aforementioned factors controlled sediment gravity flow deposition. This Formation groups mixed calciclastic, siliciclastic and volcaniclastic turbidite successions deposited in the late Paleogene - early Neogene subduction zone of the Maghrebian - Southern Apennines orogenic belt, Fig. 1 (e.g. Critelli, 1993, 2018; Carminati et al., 2012; Fornelli et al., 2020; Martín-Martín et al., 2020). This study focuses on an extraordinary well-exposed stratigraphic succession cropping out at the outer border of the Lucanian Apennines whose location is shown in Fig. 2.

Stratigraphic and sedimentological studies carried out by Critelli et al. (1990) in this area proved that deposition occurred in a physiographically complex basin with sediment supplies differentiated in both time and space, while Baruffini et al. (2002) suggested the tectonic confinement influence. In order to further enhance the facies analysis of this succession, in the last few years its re-examination has been undertaken (see also Cerone et al., 2016, 2017; Cerone, 2019). On the basis of this re-examination, the main intents of the present work are (1) to provide a new high-resolution stratigraphic framework and facies scheme, and (2) to propose a new model of sedimentary evolution, in which confining topography and active tectonics play a crucial role.

The model, proposed for the investigated succession, is expected to find applicability in analogue deep-marine successions on active margins and gives new insight for the late Paleogene Southern Apennines – Maghrebide subduction depositional setting in the Central Mediterranean.

2. Geological setting

The Tufiti di Tusa Formation outcrops across the external margin of the Southern Apennines accretionary wedge, along NW-SE stretching hills to the west of the Rotondella village, near the Ionian Coast (province of Matera, Southern Italy), Fig. 2A, B, D. This sector of the chain is structurally characterized by a buried duplex system (Apulia Chain or External Thrust System, e.g. Lentini et al., 2002; Lentini and Carbone, 2014), consisting of east-verging imbricated allochthonous sheets derived from the delamination of the Meso-Cenozoic sedimentary succession of the inner continental margin of the westward subducting Apulia Platform (Fig. 2A). The hanging wall of this duplex system is represented by a thick bulk of east-verging thin skinned thrust system including Meso-Cenozoic sedimentary successions detached from their depositional domains, both internal (Sicilide Domain, at the west of the Apennine Platform) and external (Lagonegro-Molise and Irpinian domains, to the east of the Apennine Platform) e.g. Patacca and Scandone (2007 with references).

The superposition of the allochthonous sheets on the External Thrust System occurred during Late Miocene – Lower Pleistocene (e.g. Carbone et al., 2013 with references). In detail, the study section belongs to the Sicilide Unit, which represents the highest tectono-stratigraphic unit of the outcropping Southern Apennines accretionary wedge (Figs. 2 and 3). This tectono-stratigraphic unit (Rocca Imperiale Tectonic Unit in SGI, 2012) consists of Cretaceous to lower Miocene lithostratigraphic units

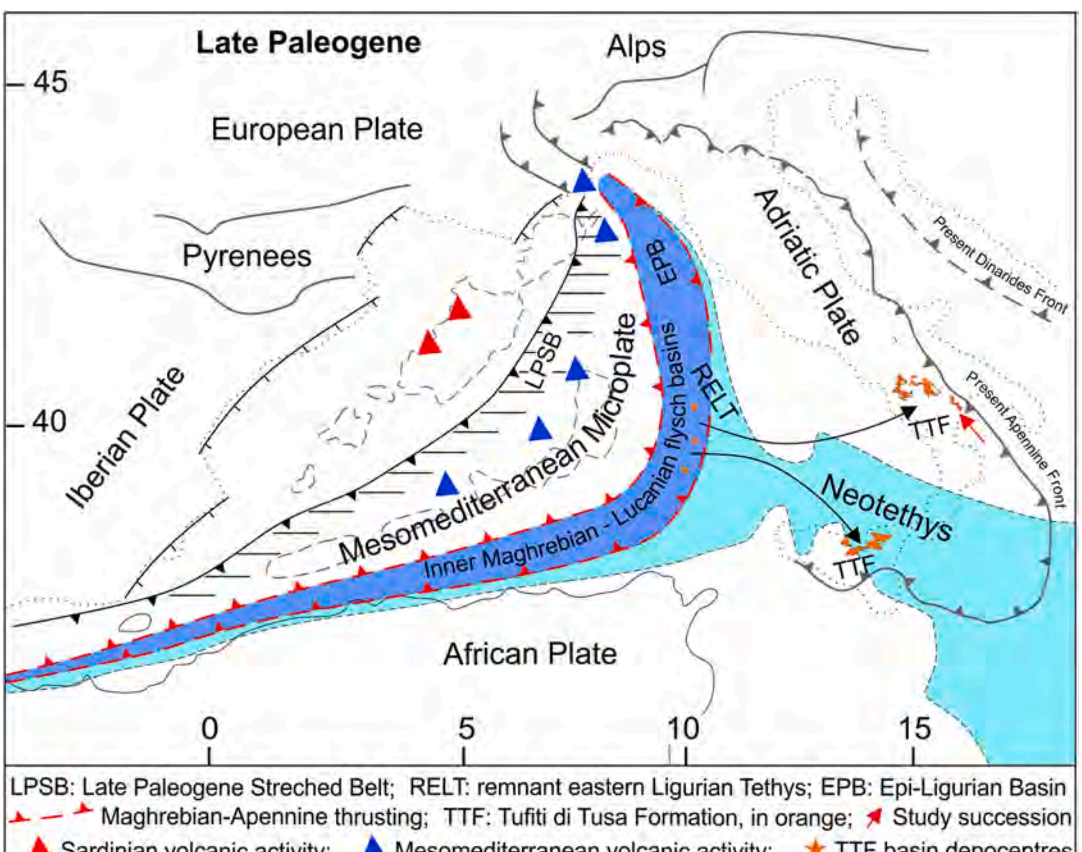

Fig. 1. Paleogeographic and paleotectonic framework of the central-western Mediterranean region during the late Paleogene (modified from Carminati et al., 2012; Fornelli et al., 2020).

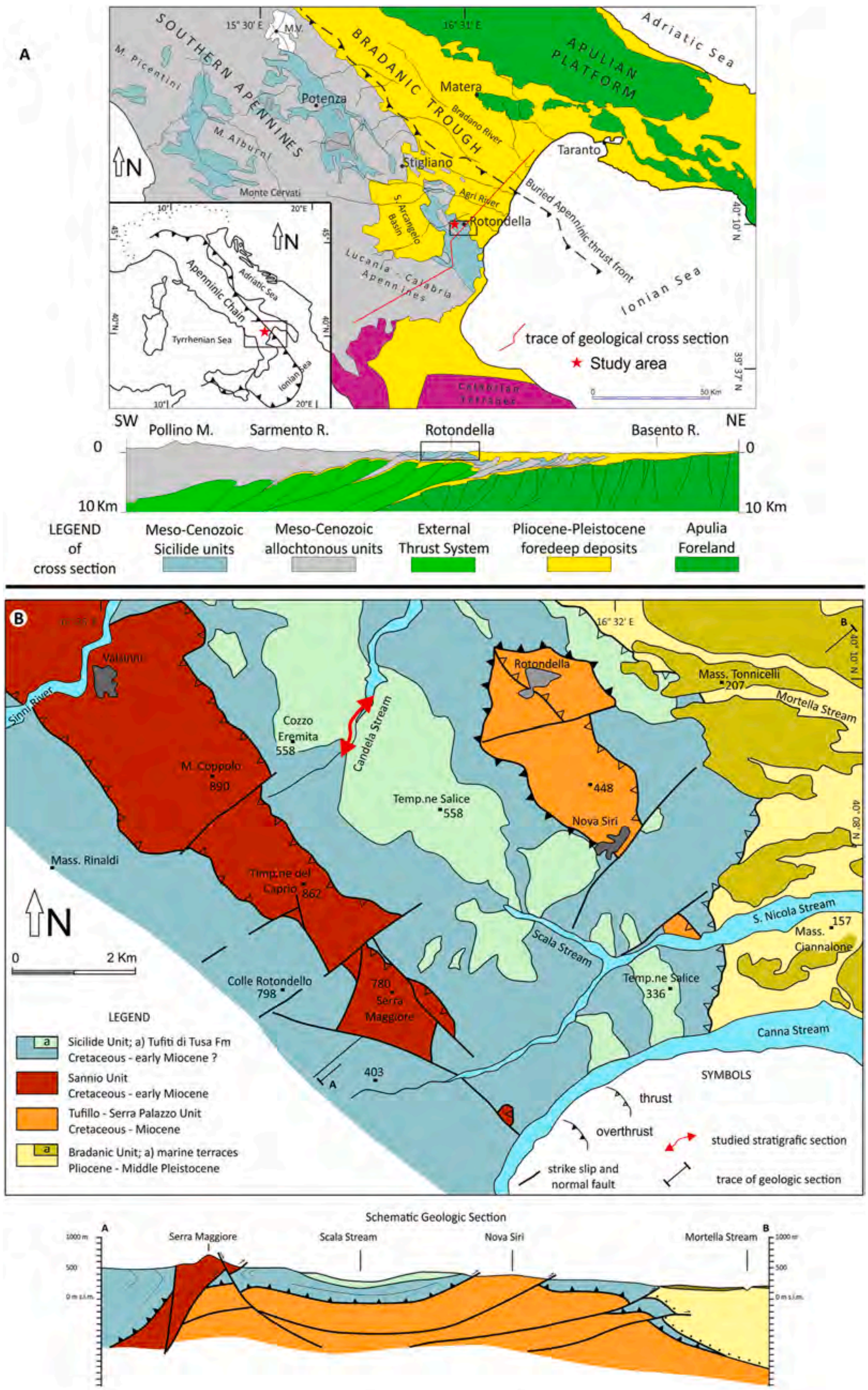

Fig. 2. A) Schematic geological map and geological cross section of Southern Italy. B) Schematic geological map and geological cross section of the south-eastern margin of the Lucanian Apennines (modified from Bonardi et al., 1988; Patacca and Scandone, 2007; SGI, 2012; Carbone et al., 2013). The location of the studied stratigraphic log of the TTF along the Candela stream is also shown.

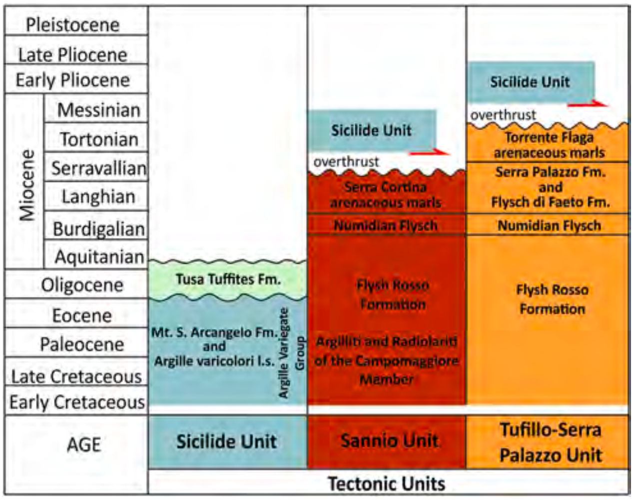

Fig. 3. Major stratigraphic features of the tectonics units of the south-eastern margin of the Lucanian Apennines (modified from Gallicchio and Maiorano, 1999; APAT, 2007; Patacca and Scandone, 2007; Sabato et al., 2007).

consisting, from bottom to top, of: i) highly deformed grey, green and red clayey deposits with thin and fine grained calciclastic and siliciclastic sandstones (Argille Variegate, Cretaceous-Eocene, Ogniben, 1969); ii) grey, green arenaceous/pelitic deep-marine clastic succession, with calciclastic, siliciclastic and volcaniclastic sandstones attributable to the Tufiti di Tusa Formation (Ogniben, 1969).

The TTF paleogeographic domain is known as the inner Maghrebian and Lucanian flysch basins, Fig. 1 (e.g. Guerrera and Martìn-Martìn, 2014) or the Sicilide Domain (e.g. Lentini and Carbone, 2014); they were located above the westward subducting oceanic lithosphere of the remnant south-eastern Tethyan oceanic realm and/or on the transitional lithosphere to the contiguous westernmost margin of the Adria Plate (e.g. Critelli, 1993; Critelli, 2018; Fornelli et al., 2022), and can reasonably be referred to a trench-slope basin (e.g. Ingersoll, 2012). The TTF source area was detailed by petrographic and U–Pb geochronology of detrital zircons studies (e.g. Critelli et al., 1990, 2017; Fornelli and Piccarreta, 1997; Perri et al., 2012; Critelli, 2018; Fornelli et al., 2020 with references). The TTF sediments mainly came from the hinterland consisting of basements involved in the Hercynian and Alpine orogens (belonging to the Mesomediterranean Microplate and the Sardinia-Corsica Block), Mesozoic sedimentary covers and a late Paleogene syn-orogenic calc-alkaline volcanic arc. Moreover, subordinate calciclastic detritus was supplied from the foreland (western carbonate platforms of the Adria Plate, e.g. Critelli, 2018; Fornelli et al., 2022). From the early Miocene, the TTF underwent several phases of thin skinned tectonic transport onto external domains of the orogen and significant rotations (e.g., Lentini et al., 2002; De Capoa et al., 2004; Speranza et al., 2003a,b).

In particular, the studied section, outcropping along the Candela Stream, lies on the western limb of a regional syncline with NW-SE striking axial plane trace, Fig. 2 (SGI, 2012; Cerone, 2019).

Although a late Oligocene - early Miocene age is generally accepted for the TTF (Patacca and Scandone, 2007; SGI, 2012), detailed biostratigraphic data and U–Pb geochronology on detrital zircons, performed along the study succession, state a late Eocene - early Oligocene age (Baruffini et al., 2002; Fornelli et al., 2020).

3. Methodology

Detailed facies analysis of the Tufiti di Tusa Formation was carried out in the type-area of the succession, along the Candela Stream located in the outer margin of the south-eastern Lucanian Apennines, Southern Italy (see Fig. 2).

A 233 m thick section of the TTF was measured and described at a scale of 1:10 by means of the following techniques: (i) bed by bed measurement using a meter stick and a Jacob's staff; (ii) analysis of the deposit composition with the aid of diluted hydrochloric acid; (iii) analysis of the grain-sizes with the aid of a grain-size comparator and a hand lens (10X); (iv) analysis of the sedimentary structures; (v) measurement of the paleocurrents indicated by sole casts and internal sedimentary structures, (vi) analysis of both dimensions and distribution of the mud-clasts.

The measured paleocurrents were successively rotated to take into account the tectonic deformation of the studied succession; particularly, an 80° clockwise rotation was applied, on the basis of the Miocene counterclockwise rotation of the southern Apennine realms, according to Gattacceca and Speranza, 2002; Speranza et al. 2003a, 2003b).

The general facies scheme considered for the facies analysis was that by Mutti et al. (2003) . However, more specific facies schemes by Tinterri and Tagliaferri (2015) and Tinterri and Piazza (2019), developed for the foredeep turbidites of the northern Apennines, have been also taken into account for developing the facies tract of this work (see below).

4. Results

4.1. Introduction

The stratigraphic section is characterized by a dip direction toward the NE and an upward dip angle decreasing from about 50° to 15°, with some rare irregular value due to minor faults (Figs. 4 and 5). The dip-angle trend can be interpreted as associated with a growth structure affecting the western margin of the basin able to produce syntectonic progressive unconformities (e.g. Riba, 1976). From a few metres to about 150 m above the base of stratigraphic section, synsedimentary asymmetrical folds and reverse fault, at outcrop-scale, were encountered.

4.2. Bed types

On the basis of texture, sedimentary organisation and distribution of the mud clasts, the beds characterizing the studied stratigraphic succession were subdivided into different types, subtypes and sub-subtypes, which are described below and interpreted in terms of interplay between confining topography and sediment gravity flows processes (see Fig. 6A, B).

4.2.1. Type 1

4.2.1.1. Description. Type 1 beds (Figs. 6 and 7) are 3.4–4.7 m-thick beds with a basal unit of 2.8–4 m-thick poorly to moderately-sorted massive to crudely-laminated very coarse to coarse/medium-grained

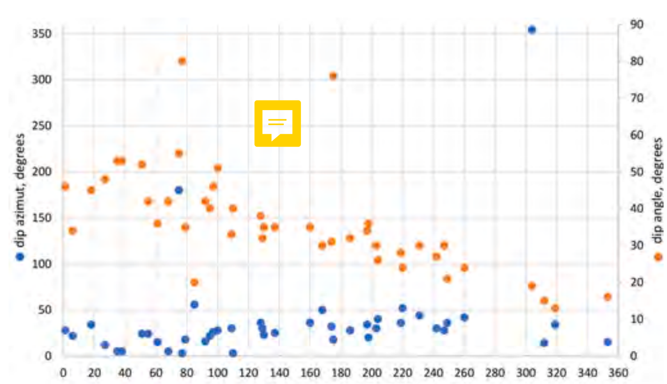

Fig. 4. Dip direction and dip angle of the beds across the study stratigraphic section.

Fig. 5. Overview of the syntectonic grow strata in the upper portion of the study section. Withe lines highlight the upward decreasing values of dip angle, ranging from about 30° to 15°. Unit III and Unit II (see 4.3 section); a: very thick Type 5.1 bed in the lower portion of Unit III; b and c: very thick Type 1 beds in the middle part of Unit III (see Figs. 6, 13).

sandstone, which can show normal grading, mud clasts and small sole casts (flutes and grooves) (facies F5 of Mutti et al., 2003). This facies (i, in Fig. 6) can pass upward into the following units: (ii) a rare unit characterized by a megaripple cross-lamination (0.20 m-thick) made of coarse to medium-grained sandstone (facies F6 of Mutti et al., 2003). (iii) a more common unit composed of fine-grained sandstone to siltstone (0.20–0.57 m-thick), which can show even and parallel to undulated lamination, convolute laminae and water escape structures (F9 of Mutti et al., 2003). (iv) A usually present unit of 0.07–0.20 m-thick massive mudstone (F9 of Mutti et al., 2003).

On the basis of occurrence of the ii unit (F6 facies), Type 1 beds can be subdivided into Subtypes 1.1 (Fig. 7A) and 1.2 (Fig. 7B), i.e. with and without F6, respectively.

The composition of facies i (F5), ii (F6), iii (sandy F9) is volcaniclastic, while facies iv (muddy F9) is argillaceous to marly.

4.2.1.2. Interpretation. Beds of this type can record flow decoupling processes between the basal decelerating dense flow (responsible for deposition of the lower thick F5) and the upper bypassing turbulent flow. The bypass of the upper turbulent part of the same flow can produce traction facies F6, while the thin F9 can be interpreted as deposited by the tail of the bypassed flow. The flow deceleration could be triggered or enhanced by morphological obstacles and basin confinement. The above interpretation matches that of similar beds, such as Type C beds by Tinterri and Tagliaferri (2015) and Type 1 beds by Tinterri and Piazza (2019) belonging to the Marnoso-arenacea and Cervarola Sandstone formations (Northern Apennines, Italy), respectively.

4.2.2. *Type 2*

4.2.2.1. Description. This type includes thick to very thick beds, consisting of volcaniclastic well-sorted medium sandstone with crude lamination (i unit in Fig. 6, corresponding to F8 of Mutti et al., 2003). Generally, these bed types are devoid of the upper fine grained laminated F9 facies (i.e. Tbe divisions, see Figs. 6 and 7B).

4.2.2.2. Interpretation. Type 2 beds can be interpreted in a similar way to Type 1 beds. These beds can indeed record flow decoupling between the basal decelerating high density part of the flow (responsible for deposition of the lower thick F8) and the upper bypassing turbulent part of the same flow able to transport more down-current fine-grained sand to mud (i.e. grain size population D in Fig. 6). In particular, F8 facies can be related to high rates of fallout from a turbulent flow (Mutti et al., 2003). Also in this case the decoupling process could be triggered or enhanced by morphological obstacles and basin confinement. The above interpretation matches very well Type D beds by Tinterri and Tagliaferri (2015) belonging to the Marnoso-arenacea Formation (Northern Apennines, Italy).

4.2.3. *Type 3*

4.2.3.1. Description. These beds (Figs. 6, 8 and 9) are characterized by the facies listed below from base to top:

(i) A rare (relatively thin) decimetric-thick unit of poorly-sorted very coarse to coarse/medium-grained sandstone, which can show mud clasts with maximum size up to a few decimetres, small flute and load casts (F5 by Mutti et al., 2003).

(ii) A rare 0.2 to 0.3 m-thick unit of thin traction carpets of coarse to medium-grained sandstone (F7 by Mutti et al., 2003), which can pass upward in to ripples cross-lamination of coarse to medium-grained sandstone (F6 by Mutti et al., 2003). These structures are sometimes separated by thin silty or muddy layers from the underlying massive coarse-grained intervals.

(iii) A rare up to 0.6 m-thick unit of well-sorted massive to crudely-laminated medium to medium/fine-grained sandstone (F8 by Mutti et al., 2003). When this facies forms the base of the bed, it can be characterized by small flute casts.

(iv) An ever-present, up to 2 m-thick unit of fine-grained sandstone to siltstone. Internally, this unit commonly shows a sequence of intervals with different sedimentary structures, such as parallel to undulated lamination, biconvex ripples with cross-laminae, hummocky-type structures, convolute laminations, water escape and load structures. Sometimes laminasets characterized by an abrupt increase in grain-size can also be common (Fig. 6). When this unit forms the base of the bed, other possible features are small sole casts (flutes and grooves) indicating paleocurrent directions different from those of the internal sedimentary structures, which, in their turn, can be different from one another other by as much as 180° (Fig. 8A). Trace fossils, such as Chondrites and Paleodyction, are common at the top. In this, facies "iv" is quite different from the classic Tbcd Bouma divisions; nevertheless, in term of grain sizes and type of sedimentary structures, it can be seen as an F9 facies by Mutti et al. (2003).

(v) A common 0.02 to 4.80 m-thick unit of massive mudstone, here ascribed to the F9 by Mutti et al. (2003).

Facies i (F5), ii (F6, F7), iii (F8) and iv (sandy F9) have siliciclastic,

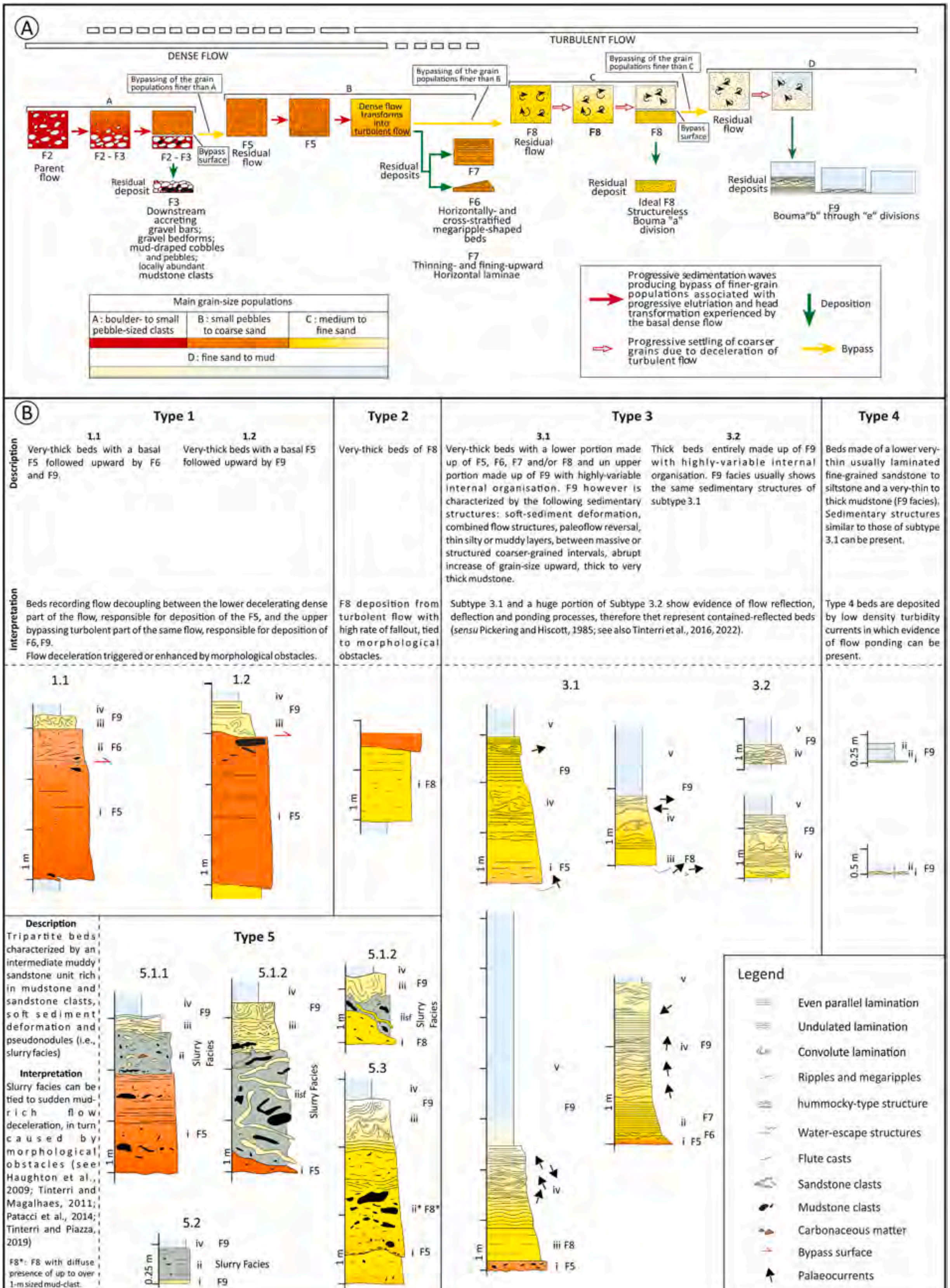

Fig. 6. A) Facies scheme considered in this paper (from Mutti et al., 2003). B) Summary of the different bed types in the study succession with their description and interpretation. This facies scheme can be compared to those by Tinterri and Tagliaferri (2015) and Tinterri and Piazza (2019) for the foredeep turbidites of the Northern Apennines.

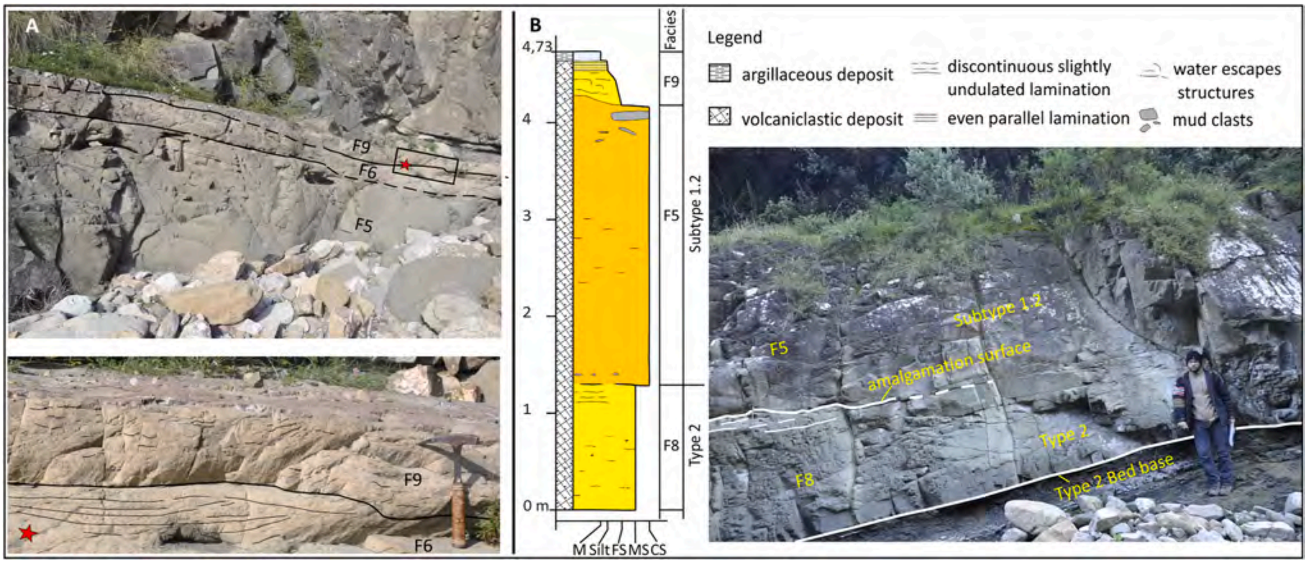

Fig. 7. A) Example of Subtype 1.1 bed. B) Stratigraphic log and photo showing an example of a Type 2 bed separated from an overlying Subtype 1.2 bed by an erosional surface.

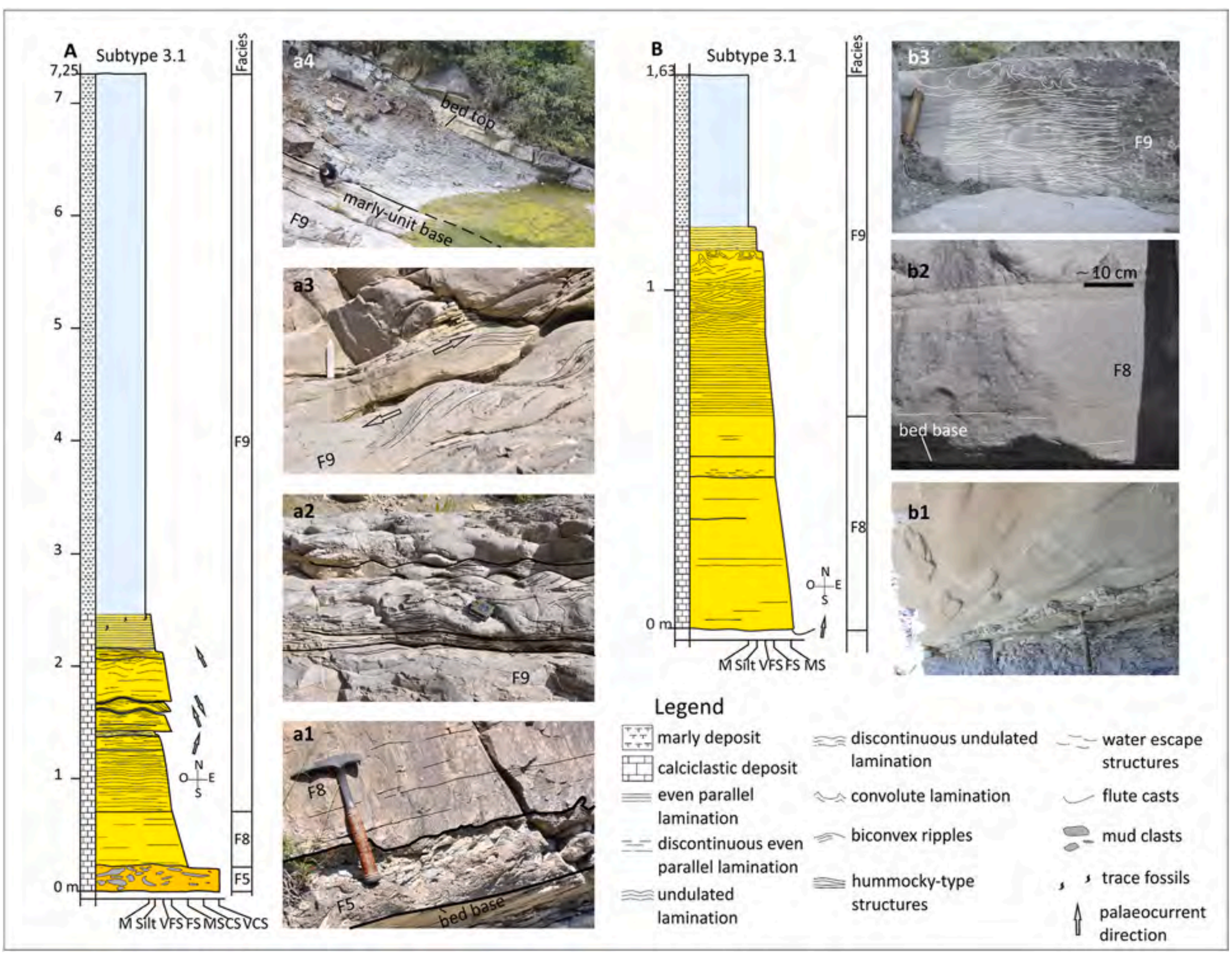

Fig. 8. A) Stratigraphic Log of a Subtype 3.1 bed. This is the thickest bed of the log and shows a facies sequence similar to that of the Contessa key bed in the Marnoso-arenacea Formation (see Tinterri et al., 2022, their Fig. 15). In the photos, the following details can be observed: basal F5 and the overlying F8 facies (a1), biconvex ripples with sigmoidal-cross laminae and small scale hummocky-type structures (a2), close-up of biconvex ripples with sigmoidal-cross laminae, showing opposite paleocurrents (a3), and panoramic view of the very-thick marly F9 at the bed top (a4). B) Log of a Subtype 3.1 bed with details on flute casts (b1), F8 facies (b2), and hummocky-type structures passing upward into convolute lamination within the F9 of the bed (b3). Worth noting is that the paleocurrents are unrotated.

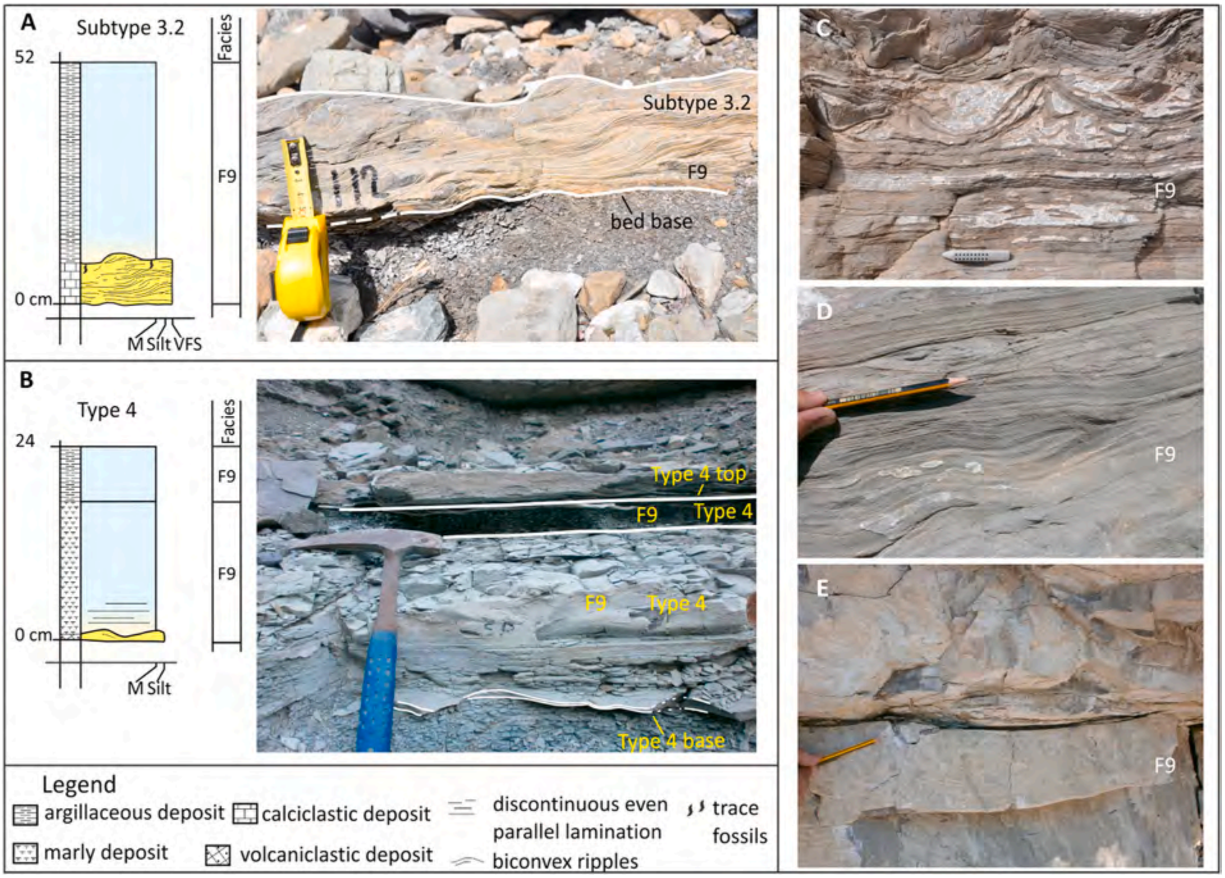

Fig. 9. A) Stratigraphic log and photo of a Subtype 3.2 bed. B) Stratigraphic log and photo of two superimposed Type 4 beds. C) Detail of even and parallel/slightly undulated lamination passing upward into load casts in a F9 facies of a Type 3 bed. D) Hummocky-type structures in a F9 facies of a Type 3 bed. E) Detail of a very-thin mud layer between coarse siltstone and very fine sandstones within a F9 of a Type 3 bed. This can be interpreted as a rebound drape by Tinterri et al. (2016, 2022).

calciclastic or volcaniclastic composition, while facies v (muddy F9) has argillaceous to marly composition.

Taking into account the presence of facies i (F5), ii (F6, F7), iii (F8), Type 3 beds are here further subdivided into the following two subtypes. (a) Subtype 3.1 beds are very thick beds characterized by one or more facies, among i (F5), ii (F6, F7) and iii (F8), Fig. 8. Much of the thickness of these bed types consists of facies iv (F9) and the upper mudstone part is often several metres thick (over 0.30 m in about 83% of cases, see Fig. 6). (b) Subtype 3.2 are thick beds consisting entirely of facies iv (F9), i.e. fine laminated sandstones that pass upwards to very thick mudstone units (over 0.30 m in about 18% of cases; see Figs. 6 and 9).

4.2.3.2. Interpretation. These bed types can be interpreted as typical contained-reflected beds in accordance with the description given by Pickering and Hiscott (1985), (see also Haughton, 1994; Remacha et al., 2005; Tinterri and Muzzi Magalhaes, 2011). In particular, facies i, ii, iii, iv and v are consistent, respectively, with facies A, B, C and D introduced by Tinterri et al. (2016, 2022) for contained-reflected beds.

Interaction between confining topography and flows can be inferred from several features of the Type 3 beds, such as biconvex ripples with sigmoidal-cross laminae, hummocky-type structures suggesting combined flows, namely flows characterized by a superimposition of an unidirectional component with an oscillatory component associated with the internal waves produced by reflection processes (e.g., Tinterri, 2011; see also Pantin and Leeder, 1987; Edwards et al., 1994; Kneller, 1995; Yokokawa, 1995; Dumas et al., 2005; Tinterri et al., 2016, 2022). Paleocurrent directions of sedimentary structures in F9 significantly differ one from the other, which is a strong indicator of flow confinement processes (e.g. Pickering and Hiscott, 1985; Kneller et al., 1991; Remacha et al., 2005; Muzzi Magalhaes and Tinterri, 2010). Load casts and convolute lamination in F9, which can be at least partially related to decelerations and reflections against morphological obstacles (Tinterri et al., 2016). Thin muddy or silty layers between massive or structured coarser layers in F9, which can be related to quiescent periods during which the turbulent flow tails drape the underlying deposits (see "rebound drapes" by Tinterri et al., 2016, 2022). In the same way, laminasets characterized by a slight increase in grain size can be attributable to a collapse of a reflected sediment wave as described by Haughton (1994) and Tinterri et al. (2022). Furthermore, thick mudstone caps can be related to flow ponding (e.g. Pickering and Hiscott, 1985; Haughton, 1994; Muzzi Magalhaes and Tinterri, 2010).

4.2.4. Type 4

4.2.4.1. Description. The beds of this type (Figs. 6 and 9) are beds consisting of the following units, in the stratigraphic up-direction: (i) a very-thin usually laminated fine-grained sandstone to siltstone (F9 of Mutti et al., 2003); (ii) a rarely-laminated thick mudstone (F9 of Mutti et al., 2003), which can be up to 0.8 cm thick with average thickness of about 0.15 m.

Unit "i" has a calciclastic, siliciclastic or volcaniclastic composition, while unit "ii" is characterized by an argillaceous to marly composition.

4.2.4.2. Interpretation. These bed types are deposited by traction plus fallout processes associated with low-density turbidity currents (Mutti et al., 2003). Nevertheless, the some-decimetres thickness of various

Type 4 beds can suggest influence of ponding processes (e.g. Pickering and Hiscott, 1985; Haughton, 1994).

4.2.5. Type 5

4.2.5.1. *Description.* Type 5 are tripartite beds with an intermediate unit that can have three different sedimentary characteristics, specifically: 1) a muddy to silty sandstone (Subtype 5.1), 2) muddy siltstone (Subtype 5.2) and 3) medium to fine-grained sandstone with abundant, up to over 1 m-sized mud clasts (Subtype 5.3), (see Figs. 6, 10–12).

Subtype 5.1 beds (Figs. 10 and 11) are 0.3–5 m-thick beds characterized by four units, which, from base to top, are: (i) A common unit of either 0.1 to 2 m-thick massive to crudely-laminated very coarse to coarse/medium-grained sandstone with possible normal grading, mud clasts, small flutes and grooves casts (F5 by Mutti et al., 2003) or about 0.5 m-thick well-sorted medium to fine-grained sandstone, where water escape structures and organic matter can be common (F8 by Mutti et al., 2003).

(ii) An always present unit of 0.4–4.5 m-thick ungraded to crudely-graded silty to muddy sandstone recording a typical slurry facies (SF) (i.e., H2 division by Haughton et al., 2009 or "B" division by Muzzi Magalhaes and Tinterri, 2010). It shows mm-to cm-sized mud clasts (Sub-subtype 5.1.1) sometimes associated with decimetric to metric more or less contorted sandstone and mudstone clasts representing bed fragments eroded from the substrate (Sub-subtype 5.1.2). Both the small mud clasts and the larger bed fragments are typically randomly distributed. In the intermediate slurry facies of both Subtype 5.1.1 and Subtype 5.1.2, water escape structures, organic matter and pseudonodules can also be observed.

(iii) An almost always present unit of 0.1–0.9 m-thick fine-grained sandstone to siltstone mainly consisting of even to undulated and parallel laminations passing upward into convolute lamination; this facies can be seen as an F9 by Mutti et al. (2003). At the base of this facies, load casts can be very common.

(iv) An always present unit of massive mudstone (F9 by Mutti et al., 2003).

Facies i (F5 and F8), ii (SF) and iii (F9) have siliciclastic or volcaniclastic composition, while the upper mudstone facies "iv" has an argillaceous to marly composition.

Subtype 5.2 beds are 0.3–0.6 m-thick beds characterized by 4 units,

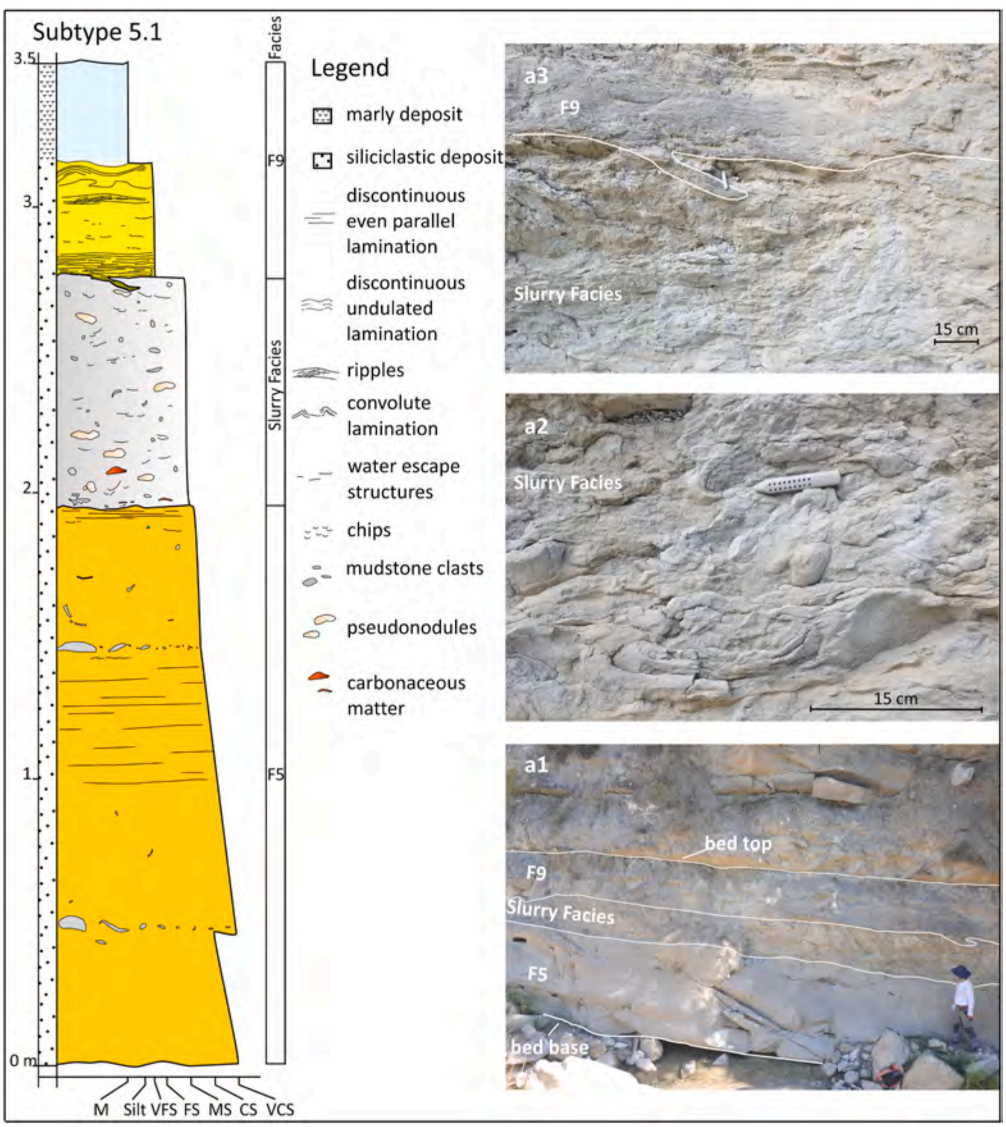

Fig. 10. Log of a Subtype 5.1 bed characterized by an intermediate slurry facies made of silty sandstone. (a1) Panoramic view of the bed from base to top; (a2) detail of the slurry facies with pseudonodules and mud clasts; (a3) detail of the slurry facies passing upwards into the F9 featuring an injection structure.

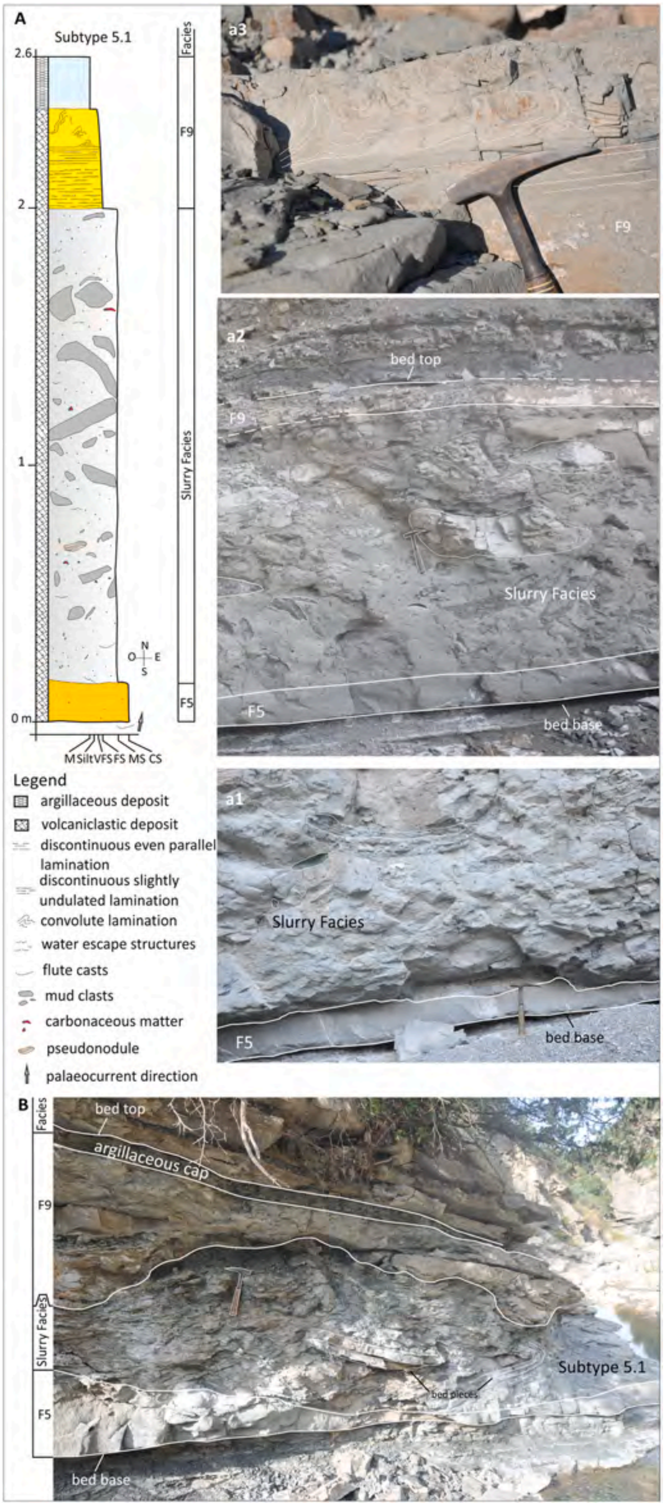

Fig. 11. A) Stratigraphic log of a tripartite Subtype 5.1 bed. The photo on the right shows the following details: F5 and Slurry Facies (a1), general view of the bed from base to top (a2), discontinuous even and parallel lamination passing upward into convolute lamination within the uppermost sandy F9 facies (a3). Mud clasts in a1 and a2 are highlighted with a red line drawing. B) Example of a Subtype 5.1 bed characterized by an F5, slurry and sandy F9 Facies with volcaniclastic composition passing upward into an argillaceous F9. Worth noting is the irregular boundary between the basal F5 and the intermediate slurry unit (where sandstone and mudstone clasts can be observed) and the load structures of the upper sandy F9. (For interpretation of the references to colour in this figure legend, the reader is referred to the Web version of this article.)

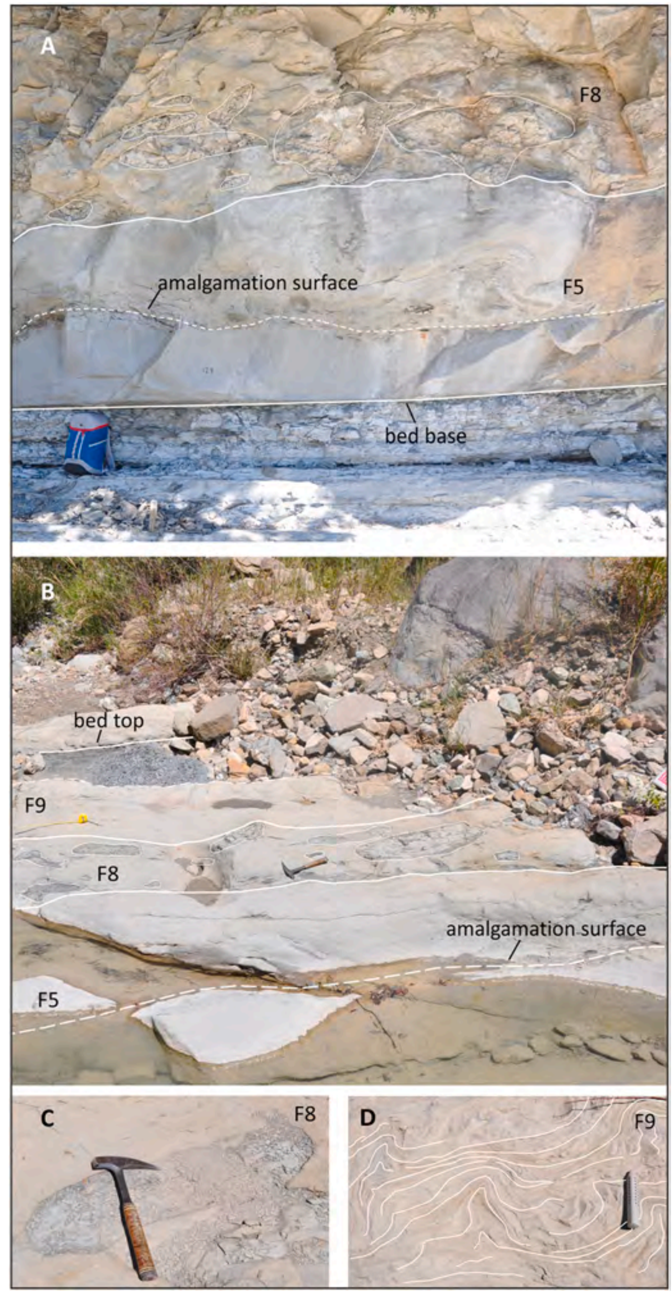

Fig. 12. A) Photo showing the lower portion of the Subtype 5.3. B) General view of the same bed shown in A. C) Large mud clasts in the F8 facies. D) Convolute lamination in the F9 facies. Mud clasts in A and B are highlighted with a white line drawing.

which, from base to top, are:

(i) An up to 0.2 m-thick always present unit made of very fine-grained sandstone to siltstone showing mud clasts and water escape structures.

(ii_{sf}) An always present unit of muddy siltstone, in which small mud clasts, organic matter, water escape structures can be observed. This unit is here referred as a slurry facies.

(iii) A sometimes present unit of 0.15 m-thick siltstone with convolute lamination.

(iv) An always present m-thick unit composed of a massive mudstone.

Facies i, iii and iv have sedimentary characteristics similar to the F9 facies by Mutti et al. (2003). The sandy and slurry facies composition is siliciclastic or volcaniclastic, while the upper mudstone unit "iv" has an argillaceous to marly composition.

Subtype 5.3 (Fig. 11) is represented by very thick beds consisting, from base to top, of the following units:

(i) A basal part composed of normally graded coarse to coarse/medium-grained sandstone with water escape structures, mud clasts up to a few tens of decimetres in size (F5 of Mutti et al., 2003). This facies can be amalgamated with underlying similar

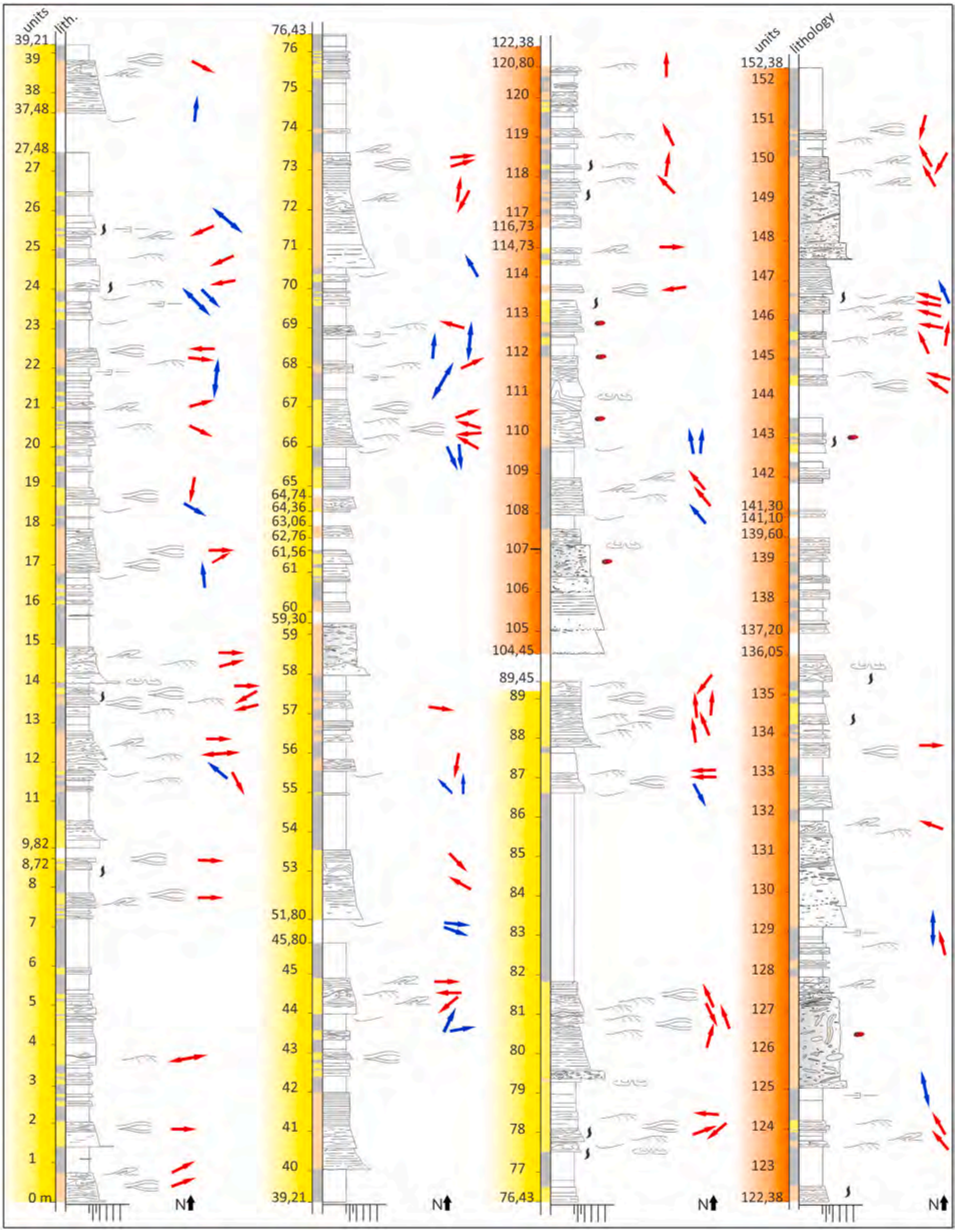

Fig. 13. Stratigraphic log of the Tufiti di Tusa Formation cropping out along the Candela stream. Noteworthy is the fact that the sandstone to siltstone deposits can have impure composition (see Fig. 2B for the location of the log).

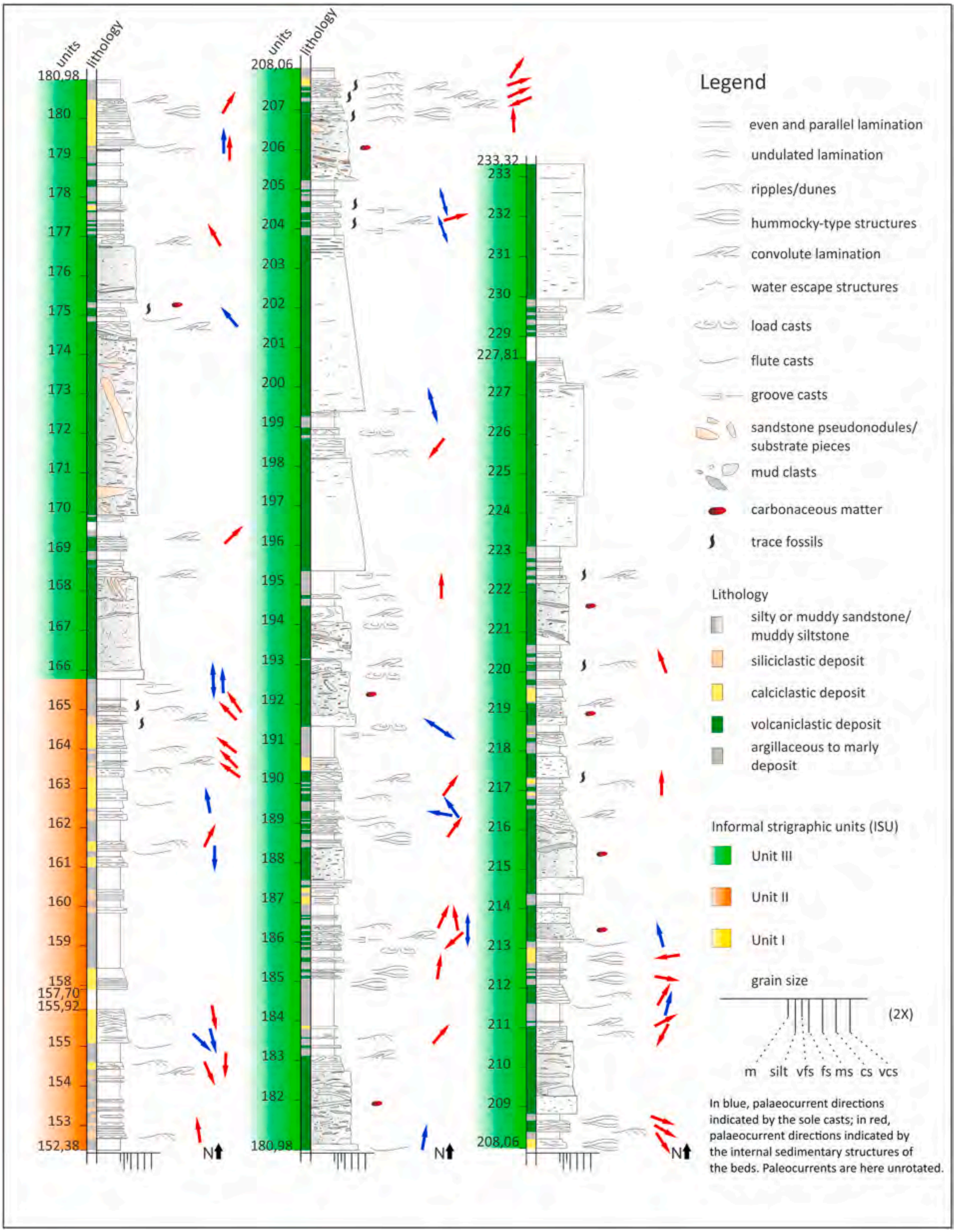

Fig. 13. (*continued*).

beds, through amalgamation surfaces marked by mudstone clast alignments.

(ii) An up to over 1 m-thick unit composed of graded medium to fine-grained sandstone, characterized by water escapes and large mud clasts with size up over 1 m with composition resembling the bed substrate (F8 by Mutti et al., 2003).

(iii) A unit of over 1 m-thick graded fine to very fine-grained sandstone, characterized, from base to top, by undulated lamination, water escape structures, slightly undulated lamination, ripples and convolute lamination (sandy F9 facies by Mutti et al., 2003).

(iv) Lastly, a unit of about 0.30 m-thick massive mudstone.

Facies “iii” and “iv” are similar to facies F9 by Mutti et al. (2003).

The facies i, ii and iii (i.e.,F5, F8 and sandy F9, respectively) have a siliciclastic composition, while the upper muddy F9 (i.e., the facies iv) has an argillaceous composition.

4.2.5.2. Interpretation. The facies sequences of Subtypes 5.1 and 5.2 closely resemble those of beds widely discussed in the last decades and identified with various terms, such as sandwich beds, slurry beds, hybrid event beds, debrites, and so on; in this paper they are termed slurry beds. According to several authors (e.g., Ricci Lucchi, 1980; Talling et al., 2004; Amy et al., 2006; Haughton et al., 2009; Sumner et al., 2009; Muzzi Magalhaes and Tinterri, 2010; Baas et al., 2011; Kane and Porten, 2012; Fonnesu et al., 2015; Southern et al., 2017; Spychala et al., 2017; Dodd et al., 2022), slurry beds could be related to erosion of muddy-substrates. Flows responsible for slurry-facies deposition can derive from flow transformation favoured by surplus of eroded mud and/or sudden flow deceleration due to morphological obstacles (e.g. Muzzi Magalhaes and Tinterri, 2010; Patacci et al., 2014; Tinterri et al., 2016, 2020; Tinterri and Piazza, 2019).

Subtype 5.3, which includes an intermediate facies F8 by Mutti et al. (2003) with abundant up to 1 m-sized mud clasts, can be interpreted as sandwich bed related to intense erosive processes (see Mutti and Nilsen, 1981; Ricci Lucchi and Valmori, 1980; Talling et al., 2004) and consequently as representing a transitional stage towards well-developed tripartite slurry beds consisting of subtypes 5.1.1 and 5.1.2 (e.g., Muzzi Magalhaes and Tinterri, 2010; Baas et al., 2011; Tinterri and Tagliaferri, 2015; Fonnesu et al., 2015).

4.3. Stratigraphy

The measured section of the Tufiti di Tusa Formation (Figs. 2 and 13; 14; and Tables 1 and 2) lies unconformably on the Argille Variegate Group. It is about 233 m-thick and shows an overall coarsening and thickening upward trend. Based on the differences in its compositional and depositional features three informal lithostratigraphic units can be distinguished, as illustrated below (Fig. 13; 13 continued).

4.3.1. Unit I

This unit represents the lower portion of the stratigraphic succession, which is about 90 m thick (see Fig. 13). Unit I has mainly-calciclastic sandstone to siltstone-fraction (Table 1A), and has a sandstone/mudstone ratio (S/M) of about 0.6 (Fig. 14A). Unit I mainly consists of facies F9 (Fig. 14C), characterized by biconvex ripples with sigmoidal laminae and hummocky-type structures and thin muddy or silty laminasets resembling the rebound drapes by Tinterri et al. (2016, 2022). Furthermore, there are significant differences in paleocurrents between sole casts and sedimentary structures within the same bed (Fig. 15) and mudstone caps with thickness ranging from some tens of decimetres to some metres (precisely 4.80 m). More precisely, paleocurrents of sole casts (flutes and grooves) of calciclastic deposits indicate flow provenance mainly from the underplate (NE) and scattered from western sectors (the latter interpreted as local deviations), while those of siliciclastic facies indicate provenance essentially from the hinterland, southwestern sector (Fig. 15). Paleocurrents of internal sedimentary structures (vergent convolute lamination, ripples and megaripples, and hummocky-type structures) of both calciclastic facies and siliciclastic facies are widely scattered (Fig. 15).

Table 1
Composition and grain-size distribution in Units I, II and III.

A		
Unit I	Relative percentage of thickness	Number
Calciclastic sandstone to siltstone intervals	31.75	80
Siliciclastic sandstone to siltstone intervals	20.68	34
Argillaceous to marly mudstone intervals	47.57	120
B		
Unit II		
Calciclastic sandstone to siltstone intervals	12.90	23
Siliciclastic sandstone to siltstone intervals	46.52	72
Argillaceous to marly mudstone intervals	40.58	94
C		
Unit III		
Calciclastic sandstone to siltstone intervals	4.64	16
Volcaniclastic sandstone to siltstone intervals	73.55	112
Argillaceous to marly mudstone intervals	21.81	118

Table 2
Minimum, maximum and mean thicknesses of the facies in Units I, II and III. Note: F9s and F9m mean sandy and muddy F9 respectively.

		Unit I	Unit II	Unit III
F5	Minimum thickness (cm)	2	9	10
	Maximum thickness (cm)	33.5	195.5	405
	Mean thickness (cm)	12.81	91.13	146.40
F6/F7	Minimum thickness (cm)	23.5	-	20.5
	Maximum thickness (cm)	34	-	20.5
	Mean thickness (cm)	28.75	-	20.5
F8	Minimum thickness (cm)	6	38	5.5
	Maximum thickness (cm)	47.5	46.5	129.5
	Mean thickness (cm)	25.19	42.25	48.25
F9s	Minimum thickness (cm)	2.5	1.5	1.5
	Maximum thickness (cm)	195.5	103.5	67.5
	Mean thickness	33.91	24.50	16.31
F9m	Minimum thickness (cm)	2	1.5	2
	Maximum thickness (cm)	480	231	120.5
	Mean thickness	27.9	21.85	12.45
Slurry Facies	Minimum thickness (cm)	108	20	19.5
	Maximum thickness (cm)	108	221	451
	Mean thickness (cm)	108	118.75	136.43

Another important feature of Unit I is the occurrence of very-thick calciclastic beds in its upper portion, including the thickest section bed, which is very similar to the “Contessa key bed” of the Marnoso-arenacea Formation in the Northern Apennines and illustrated in Fig. 8A (see also Tinterri et al., 2022).

The biconvex ripples and hummocky-type structures can be interpreted as combined flow structures, which, together with the rebound drapes and paleocurrents variations, are the basis to interpret Unit I as dominated by contained-reflected Type 3 beds (Fig. 14B) related to ponding processes in a confined basin.

4.3.2. Unit II

Unit II characterizes the intermediate part of the stratigraphic succession and is located between 105 and 165 m (the stratigraphic succession is covered for the portion between about 90 and 105 m, Fig. 13 and 13, continued). For this unit, the composition of the sandstone to siltstone-fraction is mainly siliciclastic (Table 1B), and the S/M ratio is about 0.9 (Fig. 14A). It largely consists of Type 5 beds (Fig. 14C) and Type 3 beds (Fig. 14B). The paleocurrent directions of sole casts of calciclastic deposits (mainly Type 3 beds) testify flow provenance from NE largely and SW subordinately, while those of siliciclastic deposits (mainly Type 5 beds) indicate provenance from SW (Fig. 15). The paleocurrent directions indicated by internal sedimentary structures (vergent convolute lamination, ripples and megaripples, and hummocky-type structures) of the calciclastic facies are essentially towards the eastern sectors, while those of siliciclastic facies are mainly towards the northern sectors (Fig. 15).

In comparison with the underlying Unit I, Unit II is characterized by a decrease in Type 3 beds and an increase in Type 5 beds. Regarding the

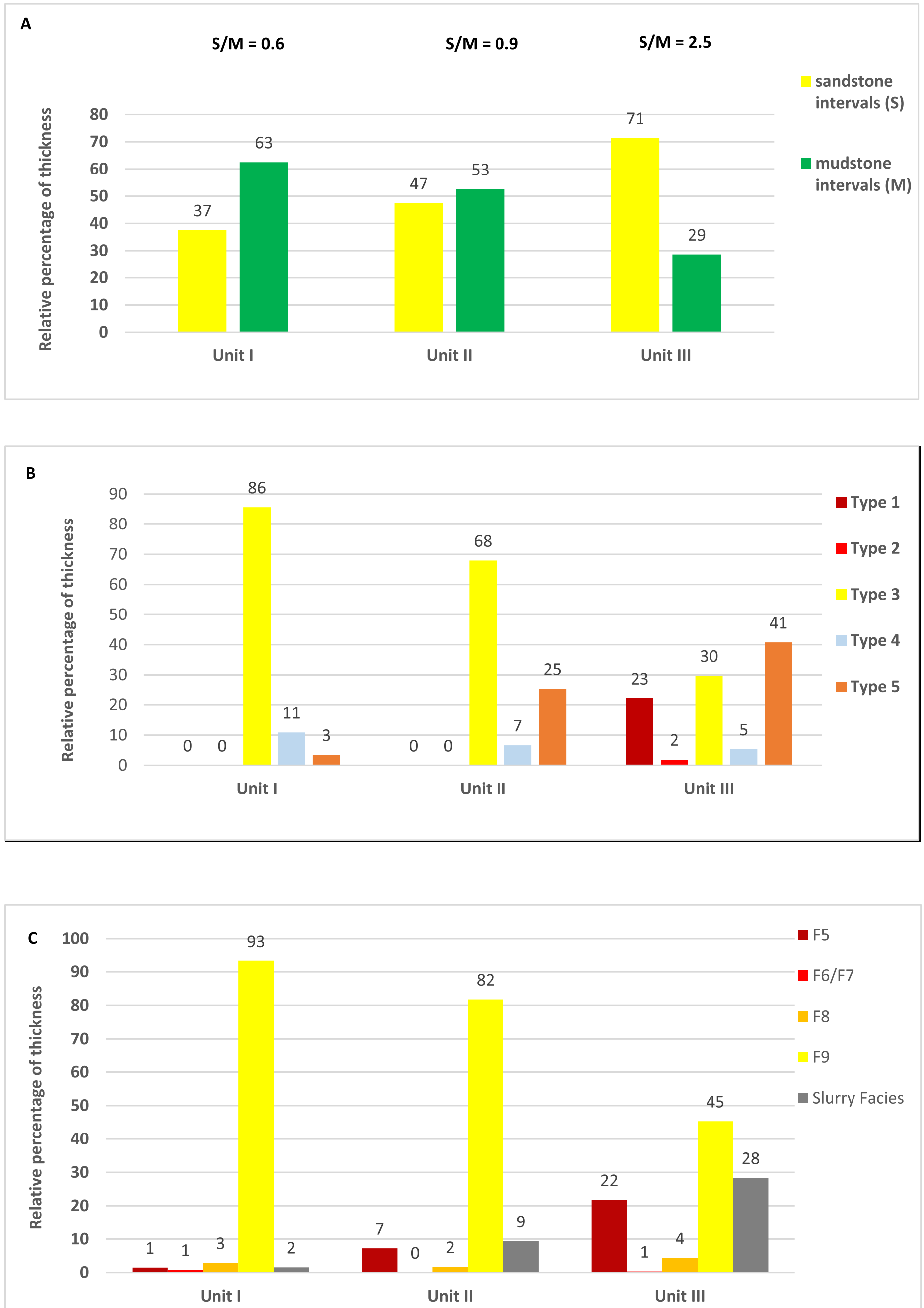

Fig. 14. A) Sandstone/mudstone ratio in Units I, II and III. B) Bed Types distribution in Units I, II and III (see Fig. 6B). C) Facies distribution by Mutti et al. (2003) in Units I, II and III (see Fig. 6A).

facies by Mutti et al. (2003), the mean thickness of F9 of Unit II is lower than the one of F9 of Unit I, whereas the mean thicknesses of F5 and F8 are higher than the ones of F5 and F8 of Unit I (Table 2). This evidence suggests that the basin confinement was still widely present during Unit II deposition. This confinement is highlighted not only by the sedimentary structures related to the ponded Type 3 beds and reversal paleocurrents (see above) but also by the occurrence of slurry Type 5 beds, which can indicate sudden mud-rich flow decelerations (e.g. Baas et al., 2009, 2011; Sumner et al., 2009; Tinterri and Piazza, 2019; Tinterri et al., 2020). These decelerations processes are also shown by an increase in massive facies represented by F5 and F8 produced by high-rate of fallout (see Tinterri and Tagliaferri, 2015; Tagliaferri and Tinterri, 2016).

4.3.3. Unit III

Unit III characterizes the uppermost part of the stratigraphic succession (from about 165 m to the section top, Fig. 13, continued). This Unit has largely-volcaniclastic sandstone to siltstone-fraction (Table 1C), and the S/M ratio of about 2.5 (Fig. 14A). Unit III essentially consists of Types 1, 3 and 5 beds (Fig. 14B) and, consequently, of slurry units and F5 facies (Fig. 14C). The mean thickness of the F9 of Unit III is lower than the one of Unit II (Table 2), whereas the mean thicknesses of the F5 and F8 are greater than ones of the F5 and F8 of Unit II (Table 2).

The only measured paleocurrent coming from a flute cast at the base of calciclastic deposits (mainly recorded by Type 3 beds) is towards the E, while measured paleocurrents of sole casts (flutes and grooves) of volcaniclastic deposits (mainly represented by Type 1 and 5 beds)

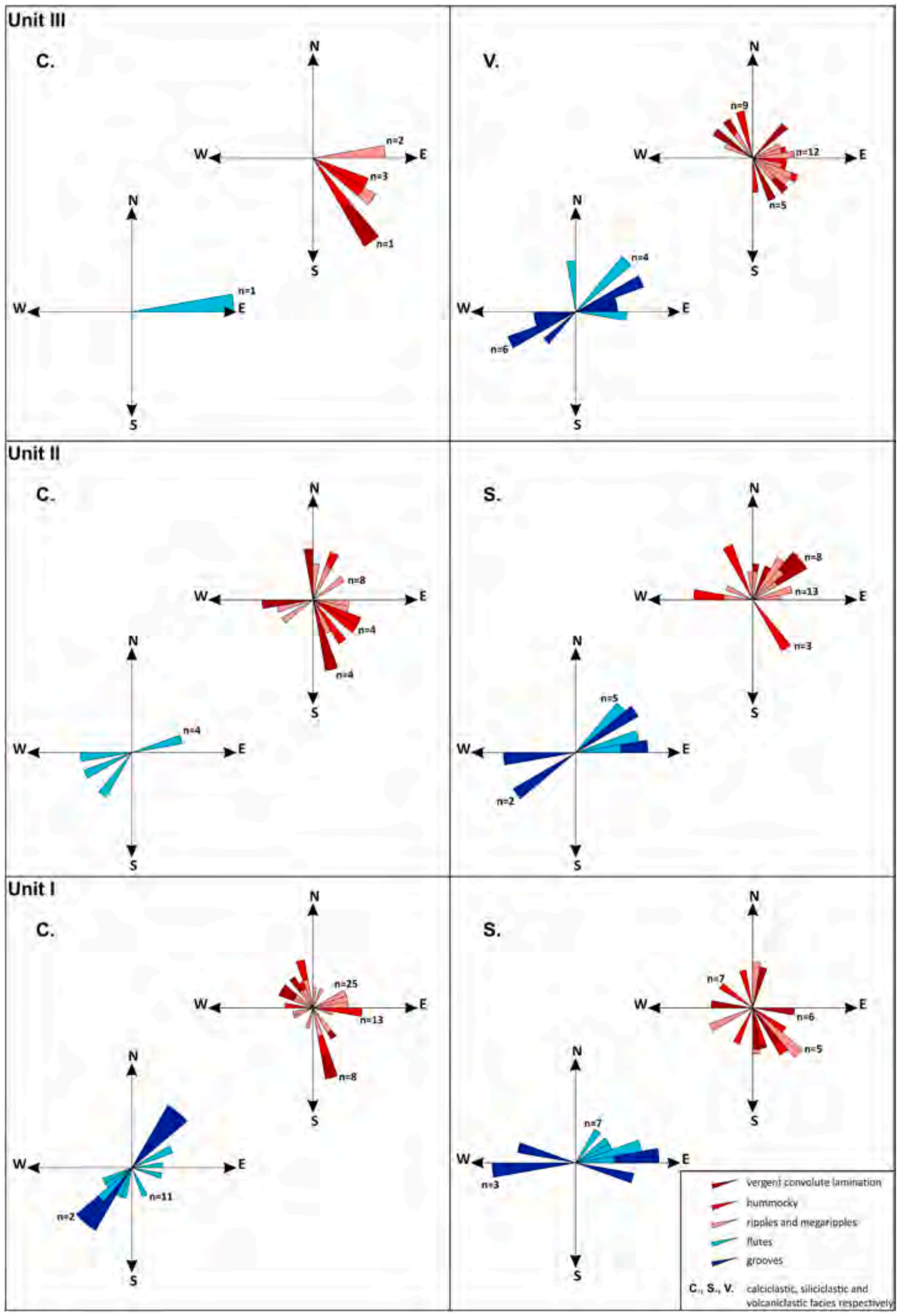

Fig. 15. Rotated paleocurrents of the studied succession.

suggest flows towards the eastern sectors (Fig. 15). Paleocurrents of internal sedimentary structures (vergent convolute lamination, ripples, megaripples, and hummocky-type structures) of calciclastic facies are towards the SE sectors, while those of volcaniclastic facies are widely scattered (Fig. 15).

A few tens of metres above the base of Unit III, a slight angular unconformity can be observed (Fig. 5), probably due to a compressive growth structure and uplift of the western margin of the basin; these may have enabled a new entry point for the volcaniclastic detritus.

In conclusion, Unit III is characterized by a drastic increase in the S/M ratio and massive and slurry facies (mainly Type 1 and 5 beds), which can indicate flow decelerations related to a confining topography. In particular, Type 1 massive beds, sometimes characterized by tractive megaripple facies (F6) at the top, can also indicate decoupling processes with the deposition of the basal dense flow to form massive facies and the bypass of the upper turbulent-flow (e.g., Mutti et al., 2003; Tinterri and Muzzi Magalhaes, 2011; Tinterri et al., 2017). Flow confinement is further demonstrated by the persistent presence of Type 3 beds, which, however, account for a lower percentage than the one in Unit II.

5. Discussion

The recognition of the turbidite basin type and the understanding of its sedimentary evolution through facies studies is one of the main objectives of recent stratigraphy and sedimentology. Detailed facies analysis, based on high-resolution physical stratigraphy of continuous stratigraphic successions, can shed light on the pivotal aspects of this issue, including the role of basin morphology and active tectonics (e.g., Sinclair, 1994; Sinclair and Tomasso, 2002; Prather, 2003; Mutti et al., 2003; Smith, 2004; Tinterri and Muzzi Magalhaes, 2011; Tinterri and Tagliaferri, 2015; Pinter et al., 2016; Bell et al., 2018; Cornard and Pickering, 2020; Cerone et al., 2021; Tinterri and Civa, 2021; McArthur and McCaffrey, 2019; McArthur et al., 2022).

The understanding of the sedimentary basin type of the TTF is considered one of the major keys for the understanding of Central Mediterranean geodynamic evolution (e.g., Guerrera and Martín-Martín, 2014; Critelli, 2018; Martín-Martín et al., 2020 with references). Indeed, this formation contains syn-orogenic volcaniclastic turbidite detritus, which testify late Paleogene – early Miocene calk-alkaline volcanic activity in the Central Mediterranean across the subduction margin of the Apennines Orogen (e.g. Critelli, 1993, 2018; Fornelli and Piccarreta, 1997; Fornelli et al., 2020). In the literature, the TTF was ascribed to different basin types, namely trench-slope basin (Lentini and Carbone, 2014), trench basin (e.g. Wezel and Guerrera, 1973) or foredeep basin (e.g. Critelli and Le Pera, 1995; Guerrera et al., 2005). These interpretations were mainly stated on the base of regional considerations and detailed petrographic analysis, rather than on high-resolution physical stratigraphy and detailed facies analysis. The data discussed in this paper, regarding the study of a stratigraphic section (singular for extension and quality of the outcrops), shed light, for the first time, on

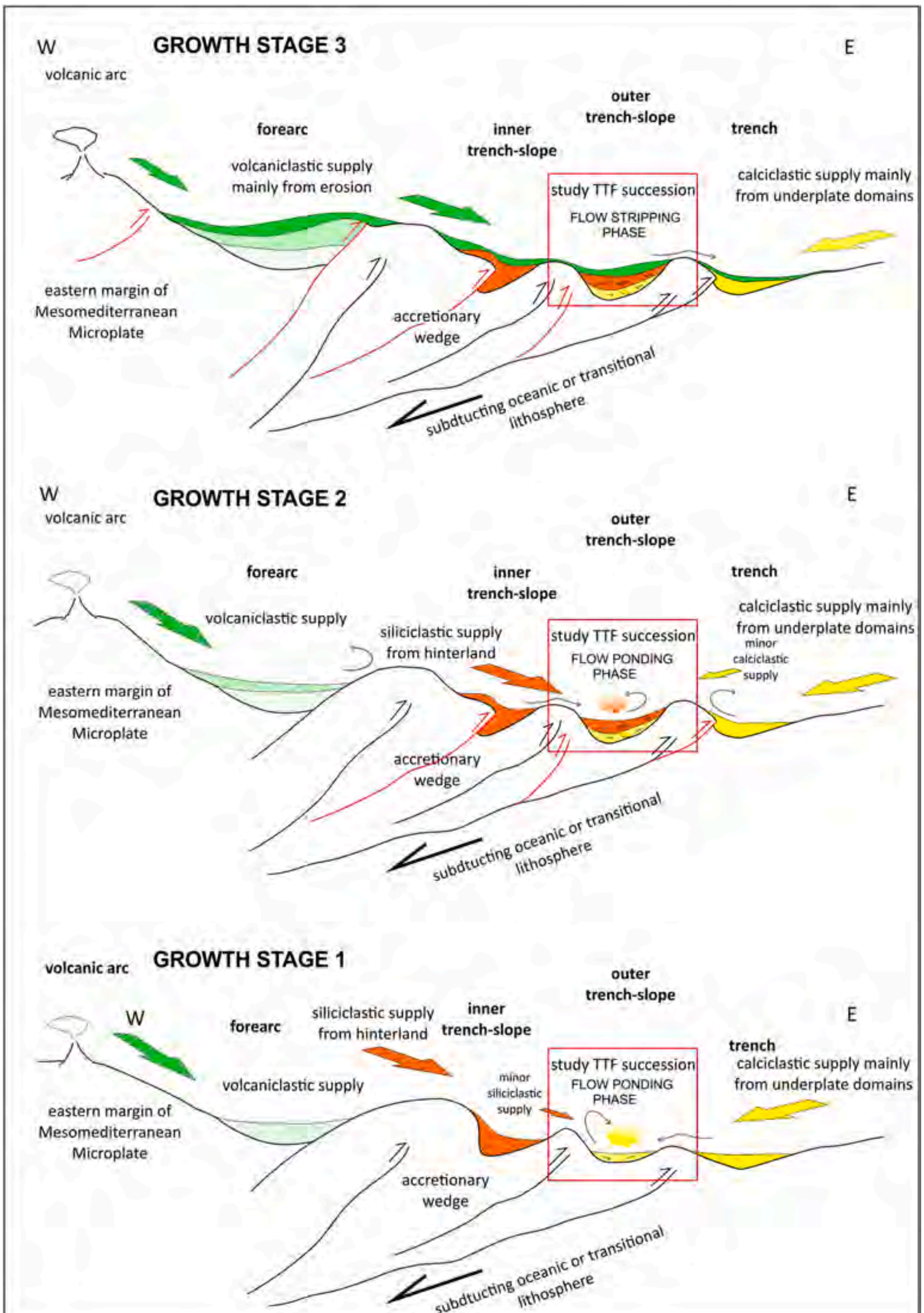

Fig. 16. Schematic representation of the depositional evolution of the studied succession in a compressional arc-trench system (see the text for details); TTF: Tufiti di Tusa Formation.

detailed distinctive depositional features. These are the basis to envisage, in accordance with regional and petrographic studies (e.g. Critelli, 2018; Guerrera et al., 2019; Fornelli et al., 2020, 2022; Martín-Martín et al., 2020), that the TTF succession in the study area (Fig. 2) could be deposited in a sub-basin of a wider trench-slope depositional system located on the late Paleogene submerged thin- skinned wedge of the Southern Apennines subduction margin.

5.1. *Depositional evolution of the TFF structurally confined basin in the study area*

Evidence of interaction between synsedimentary tectonic activity and changes in the morphology and confinement of the basin and in the sediment supply is widespread throughout the studied stratigraphic succession. This has enabled to identify three distinct lithostratigraphic units (Units I, II and III), which can record three main syntectonic growth stages (stages 1–3, Fig. 16) of the TTF study turbidite depocenter in the outer trench-slope system (*sensu* Ingersoll, 2012) of the Southern Apennines Orogen in the Central Mediterranean.

Stage 1 (Unit I) was mainly characterized by calciclastic sandstone to siltstone fed from the foreland, showing sedimentary features mostly characterized by reflected-deflected and ponding facies which reveal a strongly confined depocenter. This Unit is indeed dominated by Type 3 beds, accounting for 87% of thickness (Fig. 14B) whereas fine-grained facies F9 has high mean thickness of 52.6 cm. Furthermore, the occurrence of a Contessa-type megabed at the top of Unit 1 could be interpreted as related to syntectonic activity associated with the uplift of the outer margin of the basin which precluded calciclastic detritus from the underplate in the successive stage of its evolution. The minor siliciclastic fine-grained sandstone to siltstone beds (tab, 1), feed mainly from the southwest (Fig. 15) and feldspatholithic in composition (e.g. Critelli et al., 1990; Perri et al., 2012; Fornelli et al., 2020), could be related to flow stripping processes deriving from the up dip sub-basin of the trench-slope system and/or to distal flows through complex tectonically-controlled conduits from the hinterland.

Conversely, Stage 2 (Unit II) was marked by a sudden increase in siliciclastic supplies (mainly represented by Type 5 beds) from the hinterland. Consequently, the coarser grained sandstone and very thick slurry beds characterizing Unit II can be related to the uplift of the hinterland that favour both mud erosions and flow decelerations. However, on this point, additional effects of relative sea level changes characterizing the early Oligocene may be also supposed (see Di Capua et al., 2016 with references). More importantly, Unit II records a reduction in contained-reflected Type 3 beds and Type 4 beds (F9 facies) suggesting that, although during Unit II the incoming flows were relatively less contained in comparison with Unit I, the basin confinement was still important (see Fig. 14B and Table 2).

Lastly, Stage 3 (Unit III) characterized by multiple sediment input points is distinguishable for the sudden availability of a large amount of volcaniclastic detritus mainly represented by Type 1, 2 and 5 beds. Consequently, the widespread occurrence of slurry, coarse-grained massive sandstone beds and bypass facies with a concomitant decrease in Type 3 and 4 beds (see Fig. 14) suggests that the flow confinement degree must favour decoupling processes of bipartite flows with the deceleration and deposition of the basal dense part of the flows and the bypass and stripping of the upper turbulent flows.

In particular, slurry facies in Type 5 beds are characterized by two types of composition, namely: 1) volcaniclastic and siliciclastic sandy to muddy sandstones with mud clasts having maximum size up to over 1 m, typically resembling the substrate composition and 2) volcaniclastic or siliciclastic muddy siltstones with cm-sized mud clasts. These compositions and the nature of slurry facies related to decelerations of mud-rich flows enriched in mud thanks to erosional processes of the muddy substrate (e.g. Ricci Lucchi, 1980; Talling et al., 2004; Amy et al., 2006; Haughton et al., 2009; Muzzi Magalhaes and Tinterri, 2010; Talling, 2013), may suggest an uplift and erosion of an internal penecontemporaneous volcanic arc, the increase in up dip slope gradient and sediment supply in a confined filling basin through strongly erosive and contained currents (Fig. 16). This can also be explained by assuming burial of the morphological high(s) between the volcanic arc and the TTF basin, so that the bulk of the volcaniclastic sediment deposition must occur in the TTF basin rather than in the upper and inner basin(s) (see Sinclair and Tomasso, 2002; Brunt et al., 2004, Fig. 16); an alternative or concomitant hypothesis is that volcaniclastic sediment gravity flows became funnelled into submarine conduits cutting the above morphological high(s) (Underwood and Moore, 1995; Underwood et al., 2003; McArthr and MacCaffrey, 2020). Furthermore, since Type 5 beds percentage and their mean thickness significantly increase in Unit III (Fig. 14C; Table 2) it is also possible to envisage an increase in erosive flow capacity during the deposition of this unit.

In conclusion, the vertical facies variation of the TTF stratigraphic succession (i.e., from Unit I to Unit III) records a progressive increase not only in the sandstone/mudstone ratio but also in Type 1, 2 and 5 beds and consequently in the slurry facies and coarser-grained facies of the succession, mainly represented by F5 and F8 (see Fig. 14 and Table 2); and, likewise, a concomitant decrease (in terms of both abundance and mean thickness) is also recorded in contained reflected Type 3 beds and fine-grained type 4 beds (Fig. 14C; Table 2).

On this basis, the overall vertical facies association and depositional processes evolution characterizing the three different growth stages of the study succession can be related to the progressive filling and uplift of a trench-slope depocenter, showing strong analogies with the basin fill-and-spill architecture described by Sinclair and Tomasso (2002) for confined turbidite systems and with those described for other tectonically confined basins, such as intraslope minibasins (e.g., Prather et al., 1998; Prather, 2003), wedge top basins (e.g., Tinterri et al., 2017) and foredeep settings (e.g., Tinterri and Tagliaferri, 2015; Tagliaferri et al., 2018). In particular, according to the depositional model by Sinclair and Tomasso (2002), Units I and II can reflect the first depositional phase where flows were totally to largely trapped within the basin, allowing the hypothesis that these two units can record the flow-ponding phase, while Unit III, characterized by facies indicating flow decoupling, can fit very well with the subsequent flow stripping phase (see also, Tinterri and Tagliaferri, 2015; Tinterri et al., 2017, Fig. 16). This interpretation is also supported by paleocurrent variations in Units I, II, in which the great dispersion of the paleocurrents derived from ripples, hummocky-type structures and vergent convolutes are further evidence of ponding processes of a highly-confined basin.

It is further stressed that the description and interpretation of a sedimentary succession of about 250 m representing a basin infilling, such as that in this work, can have a great value in interpreting the evolutionary history of the basin itself, as clearly demonstrated by many works deriving from the foreland basins of the Alps, Apennines and Pyrenees (e.g., Ricci Lucchi, 1986; Covey, 1986; Sinclair and Tomasso, 2002; Mutti et al., 2003). Indeed, all these works have shown that progressive closure of the foredeep due to the thrust propagations toward the outer margin of the basin produces a thickening, coarsening and shoaling-upward stratigraphic succession, where efficient basinal turbidites pass upward into turbidite-like bodies deposited by poorly efficient gravity flows in a highly structurally-confined basin. As mentioned above, this vertical evolution, clearly characterizing northern and central Apennines foredeeps, such as those of Macigno, Cervarola, Marnoso arenacea and Laga formations (see Tinterri and Muzzi Magalhaes, 2011; Tinterri and Piazza, 2019; Milli et al., 2019; Piazza and Tinterri, 2020), has strong analogies with those of intraslope and wedge top minibasins and with that characterizing the TTF in the study area.

6. Summary and conclusions

High-resolution physical stratigraphy and facies analysis of the magnificently-exposed succession of the Tufiti di Tusa Formation along the Candela Stream (Southern Italy, Lucanian Apennines, Fig. 2) enabled to propose a first reliable model of its depositional evolution, in which basin topography and active tectonics played a crucial role in controlling both sediment pathways and sedimentary processes. Moreover, the highlighted constrains provided new insight on the geodynamic framework of the syn-subduction paleogeographic domains of the southern Apennine-Maghrebide belt in the late Paleogene.

The depositional evolution of the study succession can be summarised in the three growth stages of Fig. 16. The 1st stage (Unit I) was mainly feed by calciclastic fine-grained sediments from the underplate, showing depositional features mostly characterized by contained-reflected and ponding beds, which reveal a strongly confined depocenter. The 2nd stage (Unit II) is marked by a sudden decrease in calciclastic supplies (mainly Type 3 contained-reflected beds) and a concomitant increase in siliciclastic ones mainly represented by very thick Type 5 slurry beds. This can be related to the uplift of both the eastern margin of the basin and of the hinterland; Contessa-type beds (*sensu* Tinterri et al., 2022) at the top of Unit I and the very thick slurry beds in Unit II support this hypothesis. Conversely, the suddenly huge volume of volcaniclastic supply characterizing the uppermost 3rd stage (Unit III) could be related to the uplift of inner volcanic centres and the burial of the morphological high(s) between the internal depocenters and the external ones, and/or establishment of conduits, more likely controlled by tectonics, able to cut the above mentioned morphological highs. These vertical facies variations, together with above discussed syntectonic progressive unconformities and the basin confinement evolution, suggest a progressive infill of a confined basin featuring syn-sedimentary increase in slope gradient and sediment supply from the hinterland, which can be consistent with the growth stages by Sinclair and Tomasso (2002) and Prather (2003) for intraslope minibasins (Figs. 14 and 16). More precisely, Units I and II can record the first flow ponding phase, while Unit III the subsequently flow stripping phase as shown in the depositional model of Fig. 16.

The shown results are in accordance with the regional paleogeographic domain of the TTF suggested in the current literature and corroborate the presence of a Late Paleogene arc-trench system in the Central Mediterranean, in the north-westernmost branch of Neothetys. The above results remark the importance of the classic stratigraphic and sedimentological approach for studies of basin analyses and are grounds to propose a depositional model that can be useful for successive investigations in analogue systems in outcrop and in the subsurface.

Funding information

University of Bari Aldo Moro: Geosciences PhD scholarship 31th Cycle and UPB Gallicchio -CT14- Reg.Puglia.

Declaration of competing interest

The authors declare that they have no known competing financial interests or personal relationships that could have appeared to influence the work reported in this paper.

Data availability

Data will be made available on request.

Acknowledgements

Constructive comments and suggestions by Salvatore Critelli and Adam Daniel McArthur along with advice of Editor-in-chief Massimo Zecchin are gratefully acknowledged.

References

Amy, L.A., Talling, P.J., Edmonds, V.O., Sumner, E.J., Leseur, A., 2006. An experimental investigation on sand-mud suspension settling behaviour and implications for bimodal mud content of submarine flow deposits. Sedimentology 53, 1411–1434.

APAT, 2007. Carta Geologica d'Italia 1:50,000 - Catalogo delle Formazioni - Unità tradizionali (2). Quaderni del Servizio Geologico d'Italia, serie III, n° 7, fasc. VII. S. EL.CA., Firenze, p. 382.

Baas, J.H., Best, J.L., Peakall, J., Wang, M., 2009. A phase diagram for turbulent, transitional, and laminar clay suspension flows. J. Sediment. Res. 79, 162–183.

Baas, J.H., Best, J.L., Peakall, J., 2011. Depositional processes, bedform development and hybrid bed formation in rapidly decelerated cohesive (mud-sand) sediment flows. Sedimentology 58, 1953–1987.

Baruffini, L., Lottaroli, F., Torricelli, S., 2002. Integrated high resolution stratigraphy of the lower Oligocene Tusa tuffite Formation in the calabro lucano area and sicily (southern Italy). Riv. Ital. Paleontol. Stratigr. 108, 457–478.

Bell, D., Stevenson, C.J., Kane, I.A., Hodgson, D.M., Poyatos-More, M., 2018. Topographic controls on the development of contemporaneous but contrasting basin floor depositional architectures. J. Sediment. Res. 88, 1166–1189.

Bonardi, G., D'Argenio, B., Di Nocera, S., Marsella, E., Pappone, G., Pescatore, T.S., Senatore, M.R., Sgrosso, I., Ciaranfi, N., Pieri, P., Ricchetti, G., 1988. Carta Geologica dell'Appennino meridionale in scala 1:250.000. In 74° Congr. Soc. Geol. It., Mem. Soc.Geol.It. 41 (2).

Bouma, A.H., 1962. Sedimentology of Some Flysch Deposits, a Graphic Approach to Facies Interpretation. Elsevier Co., Amsterdam, p. 168.

Bouma, A.H., 2004. Key controls on the characteristics of turbidite systems. In: Lomas, S. A., Joseph, P. (Eds.), Confined Turbidite Systems, vol. 222. Geological Society, Special Publications, London, pp. 9–22.

Brunt, R.L., McCaffrey, W., Kneller, B.C., 2004. Experimental modelling of the spatial distribution of grain size developed in a fill-and-spill mini-basin setting. J. Sediment. Res. 74, 438–446.

Carbone, S., Senatore, M.R., Pescatore, T.S., 2013. Note Illustrative Della Carta Geologica d'Italia Alla Scala 1:50.000, Foglio 523 Rotondella. ISPRA, SystemCart, Srl, Roma. https://www.isprambiente.gov.it/Media/carg/523_ROTONDELLA/Foglio.html.

Carminati, E., Lustrino, M., Doglioni, C., 2012. Geodynamic evolution of the central and western Mediterranean: tectonics vs. igneous petrology constraints. Tectonophysics 579, 173–192.

Cerone, D., 2019. La Sedimentazione Torbiditica in Bacini Confinati. Casi Studio delle Formazioni di Serra Palazzo e delle Tufiti di Tusa (Appennino Lucano, Italia Meridionale). University of Bari Aldo Moro, pp. 1–156. Unpublished PhD thesis).

Cerone, D., Gallicchio, S., Moretti, M., Tinterri, R., 2016. Contained-reflected turbidites and slurry beds in the Tufiti di Tusa formation. Examples from lucanian Apennines (southern Italy) and their significance. Rendiconti Online of the Italian Geological Society 40, 520.

Cerone, D., Gallicchio, S., Moretti, M., Tinterri, R., 2017. Vertical facies evolution of the Tufiti di Tusa Formation cropping out in the lucanian Apennines (southern Italy). Journal of Mediterranean Earth Sciences, Special Section of XIII Geosed Congress 9, 109–112.

Cerone, D., Gallicchio, S., Patacci, M., 2021. Depositional evolution of a tectonically-confined proximal-foredeep deep-marine system: Miocene serra palazzo formation (southern Apennines, Italy). Geol. J. 56 (10), 5126–5234.

Cornard, P., Pickering, K.T., 2020. Submarine topographic control on distribution of supercritical-flow deposits in lobe and related environments, middle Eocene, Jaca Basin, Spanish Pyrenees. J. Sediment. Res. 90, 1222–1243.

Covey, M., 1986. The evolution of foreland basins to steady state: evidence from the western Taiwan foreland basin. In: Allen, P.A., Homewood, P. (Eds.), Foreland Basin, IAS Special Publication, vol. 8. Blackwell Scientific, Oxford, pp. 77–90.

Critelli, S., 1993. Sandstone detrital modes in the Paleogene liguride complex accretionary wedge of the southern apennins (Italy). J. Sediment. Petrol. 63, 464–476.

Critelli, S., 2018. Provenance of Mesozoic to Cenozoic circum-Mediterranean sandstones in relation to tectonic setting. Earth Sci. Rev. 185, 624–648.

Critelli, S., Le Pera, E., 1995. Tectonic evolution of the Southern Apennines thrust-belt (Italy) as reflected in modal compositions of Cenozoic sandstone. J. Geol. 103, 95–105.

Critelli, S., De Rosa, R., Sonnino, M., Zuffa, G.G., 1990. Significato dei depositi vulcanoclastici della Formazione delle Tufiti di Tusa, Miocene inferiore, Lucania meridionale). Boll. Soc. Geol. Ital. 109, 743–762.

Critelli, S., Muto, F., Perri, F., Tripodi, V., 2017. Interpreting provenance relations from sandstone detrital modes, Southern Italy foreland region: stratigraphic record of the Miocene tectonic evolution. Mar. Petrol. Geol. 87, 47–59. https://doi.org/10.1016/j.marpetgeo.2017.01.026.

De Capoa, P., Di Staso, A., Guerrera, F., Perrone, V., Tramontana, M., 2004. The age of the oceanic accretionary wedge and continental collision in the Sicilian sector of the Maghrebian Chain. Geodin. Acta 17, 331–348.

Decelles, P.G., 2012. Foreland basin systems revisited: variations in response to tectonic settings. In: Busby, C., Azor, A. (Eds.), Tectonics of Sedimentary Basins: Recent Advances, pp. 405–426.

Di Capua, A., Vezzoli, G., Groppelli, G., 2016. Climatic, tectonic and volcanic controls of sediment supply to an Oligocene foredeep basin: the val d'Aveto formation (northern Italian Apennines). Sediment. Geol. 332, 68–84.

Dodd, T.J.H., McCarthy, D.J., Amy, L., Plenderleith, G.E., Clarke, S.M., 2022. Hybrid event bed character and distribution in the context ofancient deep-lacustrine fan models. Sedimentology 69, 1891–1926.

Dumas, S., Arnott, R.C.W., Southard, J.B., 2005. Experiments on oscillatory flow and combined flow bed forms: implications for interpreting parts of the shallow-marine sedimentary record. J. Sediment. Res. 75, 501–513.
Edwards, D.A., Leeder, M.R., Best, J.L., Pantin, H.M., 1994. On experimental reflected density currents and the interpretation of certain turbidites. Sedimentology 41, 437–461.
Fonnesu, M., Haughton, P., Felletti, F., McCaffrey, W., 2015. Short length-scale variability of hybrid event beds and its applied significance. Mar. Petrol. Geol. 67, 583–603.
Fornelli, A., Piccarreta, G., 1997. Mineral and chemical provenance in some early Miocene sandstones of the southern Apennines (Italy). Eur. J. Mineral 9, 433–447.
Fornelli, A., Gallicchio, S., Micheletti, F., Langone, A., 2020. Preliminary U-Pb detrital zircon ages from Tufiti di Tusa formation (lucanian Apennines, southern Italy): evidence of rupelian volcaniclastic supply. Minerals 10 (9), 1–24. https://doi.org/10.3390/min10090786.
Fornelli, A., Micheletti, F., Gallicchio, S., Tursi, F., Criniti, S., Critelli, S., 2022. Detrital zircon ages of Oligocene to Miocene sandstone suites of the Southern Apennines foreland basin system, Italy. J. Palaeogeogr. 11 (2), 222–237. https://doi.org/10.1016/j.jop.2022.03.004.
Gallicchio, S., Maiorano, P., 1999. Revised stratigraphy of the serra palazzo formation, a Miocene foredeep turbidite succession of the southern Apennines (Italy). Riv. Ital. Paleontol. Stratigr. 105, 287–302.
Gattacceca, J., Speranza, F., 2002. Paleomagnetism of jurassic to Miocene sediments from the apenninic carbonate platform (southern Apennines, Italy): evidence for a 60° conterclockwise Miocene rotation. Earth Planet Sci. Lett. 201, 19–34.
Guerrera, F., Martín-Martín, M., 2014. Geodynamic events reconstructed in the betic, maghrebian, and apennine chains (central-western tethys). Bull. Soc. Geol. Fr. 185, 329–341.
Guerrera, F., Martín-Martín, M., Perrone, V., Tramontana, M., 2005. Tectonosedimentary evolution of the southern branch of the western tethys (maghrebian flysch basin and lucanian ocean): consequences for western mediterranean geodynamics. Terra. Nova 17, 358–367.
Guerrera, F., Martín-Martín, M., Tramontana, M., 2019. Evolutionary geological models of the central-western peri-Mediterranean chains: a review. Int. Geol. Rev. https://doi.org/10.1080/00206814.2019.1706056.
Haughton, P.D.W., 1994. Deposits of deflected and ponded turbidity currents, Sorbas Basin, Southeast Spain. J. Sediment. Res. 64, 233–246.
Haughton, P.D.W., Davis, C., McCaffrey, W.D., Barker, S., 2009. Hybrid sediment gravity flow deposits: classification, origin and significance. Mar. Petrol. Geol. 26, 1900–1918.
Ingersoll, R.V., 2012. Tectonics of sedimentary basins, with revised nomenclature. In: Busby, C., Azor, A. (Eds.), Tectonics of Sedimentary Basins: Recent Advances. Wiley - Blackwell Publishing Ltd.
Kane, I.A., Porten, A.S.M., 2012. Submarine transitional flow deposits in the Paleogene Gulf of Mexico. Geology 40, 1119–1122.
Kneller, B.C., 1995. Beyond the turbidite paradigm: physical models for deposition and their implications for reservoir prediction. In: Hartley, A.J., Prosser, D.J. (Eds.), Characterization of Deep Marine Clastic Systems, vol. 94. Geological Society, Special Publication, pp. 31–49.
Kneller, B.C., Edwards, D., McCaffrey, W., Moore, R., 1991. Oblique reflection of turbidity currents. Geology 19, 250–252.
Lentini, F., Carbone, S., 2014. Geology of sicily. Mem. Descr.lla Carta Geol. Italia 95, 7–30.
Lentini, F., Carbone, S., Di Stefano, A., Guarnieri, P., 2002. Stratigraphical and structural constraints in the Lucanian Apennines (southern Italy): tools for reconstructing the geological evolution. J. Geodyn. 34, 141–158.
Martín-Martín, M., Guerrera, F., Tramontana, M., 2020. Geodynamic implications of the latest Chattian-Langhian central-western peri-Mediterranean volcano-sedimentary event: a review. J. Geol. 128, 29–43.
McArthur, A.D., McCaffrey, W.D., 2019. Sedimentary architecture of detached deep-marine canyons: examples from the east Coast basin of new zeland. Sedimentology 66, 1067–1101.
McArthur, A.D., Bailleul, J., Mahieux, G., Claussmann, B., Wunderlich, A., McCaffrey, W. D., 2021. Deformation–sedimentation feedback and the development of anomalously thick aggradational turbidite lobes: outcrop and subsurface examples from the Hikurangi Margin, New Zealand. J. Sediment. Res. 91 (4), 362–389.
McArthur, A.D., Crisóstomo-Figueroa, A., Wunderlich, A., Karvelas, A., McCaffrey, W.D., 2022. Sedimentation on Structurally Complex Slopes: Neogene to Recent Deep-Water Sedimentation Patterns across the Central Hikurangi Subduction Margin, New Zeland. Basin Research. https://doi.org/10.1111/bre.12686.
Milli, S., Marini, M., Moscatelli, M., 2019. The lower-middle Messinian turbidite deposits of the Laga Basin (central Apennines, Italy). Rome – Italy. In: Vigliotti, M., Tropeano, M., Pascucci, V., Ruberti, D., Sabato, L. (Eds.), Field Trips - Guide Book; F I E L D T R I P B5b, 34th IAS Meeting of Sedimentology. September 10-13 2019, p. B5b-1/B5b-14.
Morris, S.A., Alexander, J., 2003. Changes in flow direction at a point caused by obstacles during passage of a density current. J. Sediment. Res. 73, 621–629.
Mulder, T., Alexander, J., 2001. Abrupt change in slope causes variation in the deposit thickness of concentrated particle-driven density currents. Mar. Geol. 175, 221–235.
Mutti, E., Nilsen, T.H., 1981. Significance of intraformational rip-up clasts in deep-sea fan deposits. Int. Assoc. Sedimentol. 2nd Eur. Reg. Meet. 117–119. Bologna.
Mutti, E., Tinterri, R., Benevelli, G., Di Biase, D., Cavanna, G., 2003. Deltaic, mixed and turbidite sedimentation of ancient foreland basins. Mar. Petrol. Geol. 20, 733–755.
Muzzi Magalhaes, P., Tinterri, R., 2010. Stratigraphy and depositional setting of slurry and contained (reflected) beds in the Marnoso-arenacea Formation (Langhian-Serravallian) northern Apennines, Italy. Sedimentology 57, 1685–1720.
Ogniben, L., 1969. Schema introduttivo alla geologia del confine calabro-lucano. Memor. Soc. Geol. Ital. 8, 453–763.
Pantin, H.M., Leeder, M.R., 1987. Reverse flow in Turbidity currents: the role of internal solitons. Sedimentology 34, 1143–1155.
Patacca, E., Scandone, P., 2007. Geology of the southern Apennines. In: Mazzotti, A., Patacca, E., Scandone, P. (Eds.), Results of the CROP Project Sub-project CROP-04 Southern Apennines (Italy), Bollettino Della Società Geologica Italiana, vol. 7, pp. 75–119.
Patacci, M., Haughton, P.D.W., McCaffrey, W.D., 2014. Rheological complexity in sediment gravity flows forced to decelerate against a confining slope, Braux, SE France. J. Sediment. Res. 84, 270–277.
Patacci, M., Haughton, P.D.W., McCaffrey, W.D., 2015. Flow behaviour of ponded turbidity currents. J. Sediment. Res. 85, 885–902.
Perri, F., Critelli, S., Cavalcante, F., Mongelli, G., Sonnino, M., Dominici, R., De Rosa, R., 2012. Provenance signatures for the Miocene volcaniclastic succession of the tufiti di Tusa formation, southern Apennines, Italy. Geol. Mag. 149, 423–442.
Piazza, A., Tinterri, R., 2020. Cyclic stacking pattern, architecture and facies of the turbidite lobes in the Macigno sandstones formation (chattian- aquitanian, northern Apennines, Italy). Mar. Petr. Geology 122, 104704.
Pickering, K.T., Hiscott, R.N., 1985. Contained (reflected) turbidity from the middle ordovician cloridorme formation, quebec, Canada: an alternative to the antidune hypothesis. Sedimentology 32, 373–394.
Pickering, K.T., Hiscott, R.N., 2015. Deep Marine Systems - Processes, Deposits, Environments, Tectonics and Sedimentation. Wiley-Blackwell, p. 672.
Pinter, P.R., Butler, R.W.H., Hartley, A.J., Maniscalco, R., Baldassini, N., Di Stefano, A., 2016. The Numidian of Sicily revisited: a thrust influence confined turbidite system. Mar. Petrol. Geol. 78, 291–311.
Prather, B.E., 2003. Controls on reservoir distribution, architecture and stratigraphic trapping in slope settings. Mar. Petrol. Geol. 20, 529–545.
Prather, B.E., Booth, J.R., Steffens, G.S., Craig, P.A., 1998. Classification, lithologic calibration, and stratigraphic succession of seismic facies of intraslope basins, deep-water Gulf of Mexico. AAPG Bull. 82 (5A), 701–728.
Remacha, E., Fernandez, L.P., Maestro, E., 2005. The transition between sheetlike lobe and basin-plainturbidites in the Hecho basin (South-Central Pyrenees, Spain). J. Sediment. Res. 75, 798–819.
Riba, O., 1976. Syntectonic unconformities of the Alto cardener, Spanish Pyrenees: a genetic interpretation. Sediment. Geol. 15, 213–233.
Ricci Lucchi, F., 1980. Sedimentologia. Processi e meccanismi di sedimentazione Parte 2. CLUEB, p. 212.
Ricci Lucchi, F., 1986. The Oligocene to recent foreland basins of the Northern Apennines. In: Allen, P.A., Homewood, P. (Eds.), Foreland Basin, IAS Special Publication, vol. 8. Blackwell Scientific, Oxford, pp. 105–139.
Ricci Lucchi, F., Valmori, E., 1980. Basin-wide turbidites in Miocene, over-supplied deep-sea plain: a geometrical analysis. Sedimentology 27, 241–270.
Sabato, L., Gallicchio, S., Pieri, P., Salvini, G., Scotti, P., 2007. Cretaceous anoxic events in the argilliti e radiolariti di Campomaggiore unit (Lagonegro-Molise basin, southern Italy). Boll. Soc. Geol. Ital. 7, 57–74.
SGI, 2012. Carta geologica d'Italia alla scala 1:50000 foglio 523 Rotondella. In: ISPRA, SystemCart Srl. Roma. https://www.isprambiente.gov.it/Media/carg/523_ROTONDELLA/Foglio.html.
Sinclair, H.D., 1994. The influence of lateral basinal slopes on turbidite sedimentation in the Annot Sandstones of SE France. J. Sediment. Res. 64, 42–54.
Sinclair, H.D., Tomasso, M., 2002. Depositional evolution of confined turbidite basins. J. Sediment. Res. 72, 451–456.
Smith, R., 2004. Silled sub-basins to connected tortuous corridors; sediment distribution systems on topographically complex subaqueous slopes. In: Lomas, S.A., Joseph, P. (Eds.), Confined Turbidite Systems, vol. 222. Geological Society of London Special Publication, pp. 23–43.
Southern, S.J., Kane, I.A., Warchol, M.J., Porten, W., McCaffrey, W.D., 2017. Hybrid event beds dominated by transitional-flow facies: character, distribution and significance in the Maastrichtian Springar Formation, north-west Vøring Basin, Norwegian Sea. Sedimentology 64, 747–776.
Soutter, E.L., Bell, D., Cumberpatch, Z.A., Ferguson, R.A., Spychala, Y.T., Kane, I.A., Eggenhuisen, J.T., 2021. The influence of confining topography orientation on experimental turbidity currents and geological implications. Front. Earth Sci. 8, 540–633.
Speranza, F., Adamoli, L., Maniscalco, R., Florindo, F., 2003a. Genesis and evolution of a curved mountain front; paleomagnetic and geological evidence from Gran Sasso Range (central Apennines, Italy). Tectonophysics 362, 183–197.
Speranza, F., Maniscalco, R., Grasso, M., 2003b. Pattern of orogenic rotations in central-eastern Sicily: implications for the timing of spreading in the Tyrrhenian Sea. J. Geol. Soc. 160, 183–195.
Spychala, Y.T., Hodgson, D.M., Prelat, A., Kane, I.A., Flint, S.S., Mountney, N.P., 2017. Frontal and lateralsubmarine lobe fringes: comparing sedimentary facies, architecture and flow processes. J. Sediment. Res. 87, 75–96.
Sumner, E.J., Talling, P.J., Amy, L.A., 2009. Deposits of flows transitional between turbidity current and debris flow. Geology 37, 991–994.
Tagliaferri, A., Tinterri, R., 2016. The tectonically-confined firenzuola turbidite system (Marnoso-arenacea Formation, northern Apennines, Italy). It. J. Geosci. 135, 425–443.
Tagliaferri, A., Tinterri, R., Pontiggia, M., Da Pra, A., Davoli, G., Bonamini, E., 2018. Basin-scale, high-resolution three-dimensional facies modeling of tectonically confined turbidites: an example from the firenzuola system (Marnoso-arenacea Formation, northern Apennines, Italy). AAPG (Am. Assoc. Pet. Geol.) Bull. 102, 1601–1626.

Talling, P.J., 2013. Hybrid submarine flows comprising turbidity current and cohesive debris flow: deposits, theoretical and experimental analyses, and generalized models. Geosphere 9, 460–488.
Talling, P.J., Amy, L.A., Wynn, R.B., Peakall, J., Robinson, M., 2004. Beds comprising debrite sandwiched within co-genetic turbidite: origin and widespread occurrence in distal depositional environments. Sedimentology 51, 163–194.
Tinterri, R., 2011. Combined flow sedimentary structures and the genetic link between sigmoidal and hummocky-cross stratification. Geoacta 10, 43–85.
Tinterri, R., Civa, A., 2021. Laterally accreted deposits in low efficiency turbidites associated with a structurally-induced topography (Oligocene Molare Group, Tertiary Piedmont Basin, NW Italy). J. Sediment. Res. 91, 1–22. https://doi.org/10.2110/jsr.2020.174.
Tinterri, R., Muzzi Magalhaes, P., 2011. Synsedimentary structural control on foredeep turbidites: an example from Miocene Marnoso-arenacea Formation, northern Apennines, Italy. Mar. Petrol. Geol. 28, 628–657.
Tinterri, R., Piazza, A., 2019. Turbidites facies response to the morphological confinement of a foredeep (Cervarola Sandstones Formation, Miocene, northern Apennines, Italy). Sedimentology 2, 636–674.
Tinterri, R., Tagliaferri, A., 2015. The syntectonic evolution of foredeep turbidites related to basin segmentation: facies response to the increase in tectonic confinement (Marnoso-arenacea Formation, Miocene, Northern Apennines, Italy). Mar. Petrol. Geol. 67, 81–110.
Tinterri, R., Muzzi Magalhaes, P., Tagliaferri, A., Cunha, R.S., 2016. Convolute laminations and load structures in turbidites as indicators of flow reflections and decelerations against bounding slopes. Examples from the Marnoso-arenacea Formation (northern Italy) and Annot Sandstones (south eastern France). Sediment. Geol. 344, 382–407.
Tinterri, R., Laporta, M., Ogata, K., 2017. Asymmetrical cross-current turbidite facies tract in a structurally-confined mini-basin (Priabonian–Rupelian, Ranzano Sandstone, northern Apennines, Italy). Sediment. Geol. 352, 63–87.
Tinterri, R., Civa, A., Laporta, M., Piazza, A.L., 2020. Turbidites and turbidity currents. In: Scarselli, N., Jurgen, A., Chiarella, D., Roberts, D.G., Bally, A.W. (Eds.), Regional Geology and Tectonics: Principles of Geologic Analysis, second ed. Elsevier, Amsterdam, pp. 441–479.
Tinterri, R., Mazza, T., Muzzi Magalhaes, P., 2022. Contained-reflected megaturbidites of the Marnoso-arenacea Formation (Contessa key bed) and helminthoid flysches (northern Apennines, Italy) and hecho group (South-Western Pyrenees). Front. Earth Sci. 10, 1–31.
Underwood, M.B., Moore, G.F., 1995. Trenches and trench-slope basins. In: Busby, C.J., Ingersoll, R.V. (Eds.), Tectonics of Sedimentary Basins. Blackwell Science, pp. 179–219.
Underwood, M.B., Moore, G.F., Taira, A., Klaus, A., Wilson, M.E.J., Fergusson, C.L., Hirano, S., Steurer, J., 2003. Sedimentary and tectonic evolution of a trench-slope basin in the Nankai subduction zone of southwest Japan. The LEG 190 Shipboard Scientific Party. J. Sediment. Res. 73, 589–602.
Wezel, F.C., Guerrera, F., 1973. Nuovi dati sulla età e posizione strutturale del Flysch di Tusa in Sicilia. Boll. Soc. Geol. Ital. 92, 193–211.
Yokokawa, M., 1995. Combined flow ripples: genetic experiments and application for geologic records. Mem. Fac. Sci. Kyushu Univ. Ser. D Earth Planet. Sci. 29, 1–38.